inorganics

MDPI

Review

A Structural Survey of Poly-Functional Dithiocarbamate Ligands and the Aggregation Patterns They Sustain

See Mun Lee and Edward R. T. Tiekink *

Research Centre for Crystalline Materials, School of Science and Technology, Sunway University, Bandar Sunway 47500, Selangor Darul Ehsan, Malaysia; annielee@sunway.edu.my

* Correspondence: edwardt@sunway.edu.my; Tel.: +60-3-7491-7181

Abstract: An overview is presented of the crystal structures of transition metal, main group element, and lanthanide compounds containing poly-functional dithiocarbamate ligands, namely species containing two or more connected NCS_2^- residues. In all, there are 40 different ligands of this type that have been characterised crystallographically in their heavy-element compounds with up to six NCS_2^- residues; all are bridging. In most cases, the resulting aggregates are zero-dimensional, often di-nuclear, but aggregates of up to 36 metal (gold) atoms are noted. There are smaller numbers of one-, two-, and three-dimensional architectures sustained by poly-functional dithiocarbamate ligands in their respective crystals. The survey highlights the opportunities afforded by this generally under-studied class of ligand.

Keywords: thiolate ligands; dithiocarbamate ligands; coordination polymers; metal clusters; crystal structures

Citation: Lee, S.M.; Tiekink, E.R.T. A Structural Survey of Poly-Functional Dithiocarbamate Ligands and the Aggregation Patterns They Sustain. *Inorganics* **2021**, *9*, 7. https://doi.org/10.3390/inorganics9010007

Received: 17 December 2020
Accepted: 13 January 2021
Published: 15 January 2021

1. Introduction

The facile reaction between a secondary amine and carbon disulphide in the presence of an alkali metal hydroxide or ammonium hydroxide as the base leads to the formation of arguably one of the more important classes of thiolate ligands, the dithiocarbamates, formulated in its simplest form as $^-S_2CNR_2$, for R = alkyl or aryl. While it is not certain when dithiocarbamates were first prepared [1], they have most likely been around for well over 150 years based on the observation that Debus reported the synthesis of dithiocarbamic acids in 1850 [2]; subsequently, Delépine described the synthesis of metal salts of dithiocarbamates in 1907 [3]. The variety of dithiocarbamate anions that can be synthesised is limited by the number of amines available for reaction, and it can extend to primary amines and, relevant to the present survey, molecules bearing two or more amine residues giving rise to poly-functional dithiocarbamate ligands. Being a most prominent ligand in coordination chemistry, over the years, a number of authoritative reviews have summarised advances in the field of dithiocarbamate chemistry and that of their seleno-derivatives [1,4–8], with additional surveys focussing upon aspects of their structural chemistry and modes of supramolecular association in their crystals for specific groups of elements [9–14].

The importance of dithiocarbamate ligands in coordination chemistry notwithstanding, their use in expanding the burgeoning field of metal organic frameworks (MOFs) and coordination polymers is quite plainly lagging compared with, for example, the ubiquitous carboxylates [15]. This is not to suggest there is no role for sulphur in extended framework assemblies. This fact is highlighted in a few very recent reports in the literature exploring the utility of sulphur/sulphur-based ligands in this context. For example, by exploiting band gaps between p- and d-orbitals, two-dimensional metal-organosulphide arrays have long been recognised as important functional materials with applications relating to conductivity, photoluminescence, and ferro-magnetism [16–18]. The authors of a recent study exploring the utility of two-dimensional europium materials featuring Eu–S

bonds as semi-conductors and as precursors for nano-sheets query the apparent lack of sulphur-based materials in this context and conclude this may relate to the perception that metal–sulphur bonds have too much ionic character and are too labile [19]. The present authors also suggest that poor solubility may also be a perceived issue. In terms of specific dithiocarbamate ligands employed in the construction of coordination polymers, perhaps the most relevant recent study relates to a series of heterometallic, platinum(II)/zinc(II) one- and two-dimensional coordination polymers that were synthesised from multi-functional dithiocarbamate ligands featuring both dithiocarbamate and carboxylate residues [20], which were chosen for their complexation ability towards soft platinum(II) and hard zinc(II) centres, respectively. In the context of drug delivery, nanosized thiol-functionalised MOFs have been employed for the transport of the known anti-cancer (leukaemia) and anti-inflammatory drug, 6-mercaptopurine (6-MPH), to cells [21]. Here, 6-MPH was linked, via a disulphide bond, to 2,5-disulfanylterephthalate ligands within a zirconium-based MOF. In the intra-cellular environment, glutathione (GSH), which is present in a higher concentration than in extra-cellular surroundings, reduces the disulphide bond to release 6-MPH in a GSH-responsive drug-delivery strategy that results in a 3-fold efficacy of the drug [21]. In other zirconium-based MOFs, regiospecific and modular substitution in the organic staves of the framework by (thio-ether) sulphur resulted in the formation of boiling water-insensitive materials that could be subjected to controlled, post-synthetic oxidation by hydrogen peroxide [22]; it is noted that (thiophene-)sulphur can play related roles for oxygen reduction in covalent organic frameworks [23]. In one final example highlighting the potential utility of sulphur-modified MOFs, recently, thio-functionalised MOFs have been shown to be effective in bioremediation. Thus, sulphur incorporated into a zinc phosphite framework, through the agency of 2,5-thiophenedicarboxylate linkers, enabled the efficient removal of Hg^{2+} cations from aqueous solution [24].

With the above in mind, it is perhaps surprising that dithiocarbamate ligands do not appear to play a greater or even a prominent role in the construction of MOFs let alone coordination polymers. In this survey, the coordination potential of poly-functional dithiocarbamate ligands, which is defined as molecules having two or more dithiocarbamate residues, that is NCS_2^-, available for coordination, is evaluated. The survey is based on the structural data included in the Cambridge Structural Database (CSD) [25]. In all, 102 different crystals have been evaluated, revealing a total of 40 different poly-functional dithiocarbamate ligands, clearly highlighting the potential of this class of ligand. Zero-dimensional aggregation patterns predominate but, examples of one-, two-, and three-dimensional aggregates are apparent. Structures are discussed in terms of their position in the periodic table and in order of increasing nuclearity.

2. Methods

For the present bibliographic review of the crystallographic literature, the CSD (version 5.41 + three updates) [25] was searched employing ConQuest (version 2.0.4) [26]. The fragment searched for was S_2CN-spacer-NCS_2, where the spacer was zero or any element in a chain up to a maximum length of 22 atoms. No other restrictions were applied as structures with relatively high values of R and/or feature disorder can still provide reliable molecular connectivity. Indeed, disorder was often confined to solvent and/or counter-ions and sometimes modelled with the SQUEEZE routine in PLATON [27]. All retrieved structures were manually evaluated, leading to a total of 102 independent crystal structures. A total of 40 different S_2CN-spacer-NCS_2 species were identified, and the chemical diagrams for these are given in Figure 1. The full composition of each crystal is given in Table 1 along with their CSD REFCODES. All crystallographic diagrams presented herein are original and were generated with DIAMOND [28] employing data available in the deposited CIFs [25].

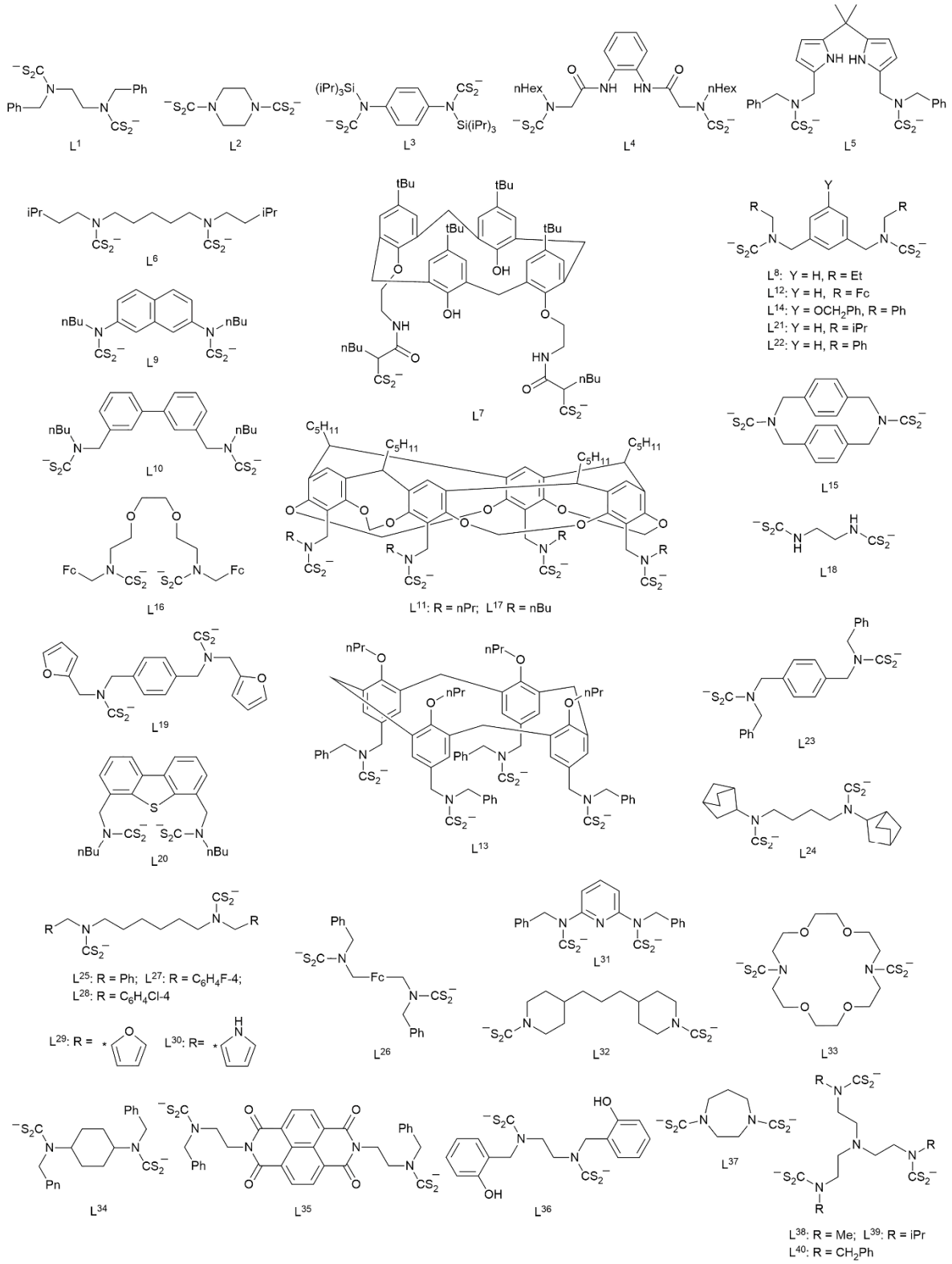

Figure 1. Chemical diagrams for poly-functional dithiocarbamate anions L^1 to L^{40}. The asterisk for each of L^{29} and L^{30} indicates the point of attachment.

Table 1. Summary of structures **1–102** covered in this bibliographic review.

Crystal	Formulation	Motif	CSD REFCODE	Ref.
1	$[Mo(=O)_2(L^1)]_2$	0-D/dimer	OFOZIS	[29]
2	$[Ru(dppm)_2]_2(L^2)$, $2(BF_4)$, $3(CHCl_3)$	0-D/dimer	QAVHAX	[30]
3	$[Cp(Ph_3P)Ru]_2(L^3)$, $1.4(C_6H_{14})$	0-D/dimer	CULLAW	[31]
4	$[(dppm)_2Ru(L^2)Pd(PPh_3)_2]$, $2(BF_4)$, $3(CH_2Cl_2)$, $C_4H_{10}O$	0-D/dimer	QONVAR	[32]
5	$[(dppe)Ni]_2(L^2)$, $2(PF_6)$	0-D/dimer	RUDLIM	[33]
6	$[(dppf)Ni]_2(L^2)$, $2(PF_6)$, $4(CH_2Cl_2)$	0-D/dimer	RUDLOS	[33]
7	$[(dppf)Ni]_2(L^1)$, $2(PF_6)$, CH_2Cl_2	0-D/dimer	ISEWEJ	[34]
8	$Ni_2(L^4)_2$, CH_3CN	0-D/dimer	ELUFOG	[35]
9	$Ni_2(L^5)_2$, $4(H_2O)$	0-D/dimer	QAHFUB	[36]
10	$[(Ph_3P)_2Pd]_2(L^2)$, $2(PF_6)$, $C_4H_{10}O$	0-D/dimer	KEKKAP	[37]
11	$[(Ph_3P)_2Pd]_2(L^2)$, $2(PF_6)$, $C_4H_{10}O$	0-D/dimer	KEKKET	[37]
12	$[(Ph_3P)_2Pd]_2(L^1)$, $2(PF_6)$, $C_4H_{10}O$	0-D/dimer	KEKKIX	[37]
13	$[(dppf)Pd]_2(L^1)$, $2(PF_6)$, CH_2Cl_2, CH_3CH_2OH	0-D/dimer	ISEWIN	[34]
14	$[(dppf)Pd]_2(L^2)$, $2(BF_4)$, $2.6(CH_2Cl_2)$	0-D/dimer	RUDLEI	[33]
15	$Pd_2(L^6)_2$	0-D/dimer	KENYIN	[38]
16	$Pd_2(L^6)_2$, $CHCl_3$	0-D/dimer	KENYOT	[38]
17	$Pd_2(L^5)_2$, $2(CH_3OH)$, $2.5(H_2O)$	0-D/dimer	QAHGAI	[36]
18	$Pd_2(L^7)_2$, $2(CH_3OH)$	0-D/dimer	IXIWAN	[39]
19	$[(Et_3P)_2Pt]_2(L^2)$, $2(PF_6)$	0-D/dimer	RUDLAE	[33]
20	$[(Ph_3P)_2Pt]_2(L^2)$, $2(PF_6)$	0-D/dimer	RUDKUX	[33]
21	$[(Ph_3P)_2Cu]_2(L^2)$	0-D/dimer	XUHYAB	[40]
22	$[(Ph_2PCH_2N(Ph)CH_2PPh_2)Cu]_2(L^2)$, $2(C_3H_7NO)$	0-D/dimer	ASANUF	[41]
23	$Cu_2(L^8)_2$, $2(FeCl_4)$, $2(C_6H_6)$	0-D/dimer	WOXFAQ	[42]
24	$Cu_2(L^9)_2$, CH_2Cl_2	0-D/dimer	GUTQIW	[43]
25	$Cu_2(L^9)_2$, ReO_4	0-D/dimer	IDEBIC	[44]
26	$Cu_4(L^{10})_2$	0-D /tetramer	GUTQES	[43]
27	$Cu_8(L^{11})_4$, $7(I_3)$, I, $6(H_2O)$	0-D/octamer	CUPLAA	[45]
28	$(Me_3PAu)_2(L^1)$	0-D/dimer	ISEWUZ	[34]
29	$(Ph_3PAu)_2(L^1)$, $2(CH_2Cl_2)$, $0.5(CH_3CH_2OH)$	0-D/dimer	ISEWOT	[34]
30	$[(Ph_3P)_2Au]_2(L^2)$, $2(CHCl_3)$	0-D/dimer	YAFMEZ	[46]
31	$[(dppf)Au_2]_2(L^2)$, $2(PF_6)$, $1.75(C_4H_{10}O)$	0-D/tetramer	PUCFAV	[47]
32	$Au_6(L^{12})_3$, $CHCl_3$	0-D/hexamer	EFARUZ	[48]
33	$Au_8(L^{13})_2$, unknown solvate	0-D/octamer	KUNCUT	[49]
34	$Au_8(L^{13})_2$, unknown solvate	0-D/octamer	KUNDAA	[49]
35	$Au_{12}(L^{14})_6$, $3(CHCl_3)$, $7(H_2O)$	0-D/12-mer	MOLMEG	[50]
36	$Au_{16}(L^{15})_4(\mu\text{-dppm})_8$, $8(BF_4)$, $2(C_2H_3N)$	0-D/16-mer	MUGJUV	[51]
37	$Au_{16}(L^2)_4(dppm)_2$, $8(PF_6)$	0-D/16-mer	TEBFEM	[52]
38	$Au_{36}(L^{12})_{18}$, $10(CHCl_3)$, $26(H_2O)$	0-D/36-mer	EFAROT	[48]
39	$Zn_2(L^{16})_2$, CH_2Cl_2, $2(H_2O)$	0-D/dimer	FIPYAF	[53]
40	$Zn_2(L^{12})_2$, CH_3CH_2OH, $0.5(H_2O)$	0-D/dimer	BAGLIF	[54]
41	$Zn_2(L^5)_2(pyridine)_2$, $2(C_5H_5N)$	0-D/dimer	QAHGEM	[36]
42	$Zn_2(L^9)_2(N(CH_2CH_2)_3N)$	0-D/dimer	FEDDOI	[55]
43	$Zn_6(L^{11})_3(pyridine)_6$, $7.5(CH_3CH_2OH)$	0-D/hexamer	CUPKUT	[44]
44	$Zn_6(L^{17})_3(pyridine)_6$, $9(CH_3CH_2OH)$, $10.5(H_2O)$	0-D/hexamer	MAKVUP	[56]
45	$[Zn(L^{18})]_n$	2-D	FUFFAQ	[57]
46	$Cd_6(L^{11})_3(pyridine)_6$, $6(CH_3CH_2OH)$, $27(H_2O)$	0-D/hexamer	MAKVOJ	[56]
47	$Cd_6(L^{17})_3(pyridine)_6$, $15(CH_3CH_2OH)$, $9(H_2O)$	0-D/hexamer	MAKVID	[56]
48	$(PhHg)_2(L^{12})$, $1.5(EtOEt)$	0-D/dimer	FUPFOM	[58]
49	$(PhHg)_2(L^{19})$	0-D/dimer	YOMXIJ	[59]
50	$Hg_2(L^{20})_2$, $2(C_2H_2Cl_4)$	0-D/dimer	XOHBAZ	[60]
51	$(Me_2Sn)_2(L^{21})_2$	0-D/dimer	BOMCOW	[61]
52	$(Me_2Sn)_2(L^{22})_2$, $2(C_6H_6)$	0-D/dimer	BOMBUB	[61]
53	$(Me_2Sn)_2(L^{23})_2$, $2(CH_2Cl_2)$	0-D/dimer	BOMCAI	[61]
54	$(Me_2Sn)_2(L^{24})_2$, $10(CDCl_3)$	0-D/dimer	SAPSAF	[62]
55	$(Me_2Sn)_2(L^{25})_2$, $2(CHCl_3)$	0-D/dimer	XONHIS	[63]

Table 1. *Cont.*

Crystal	Formulation	Motif	CSD REFCODE	Ref.
56	$(Me_2Sn)_2(L^{26})_2$, $2(CH_2Cl_2)$, $4(C_6H_6)$	0-D/dimer	BOMCEM	[61]
57	$[(nBu)_2Sn]_2(L^{25})_2$, CH_2Cl_2	0-D/dimer	XONHOY	[63]
58	$[(nBu)_2Sn]_2(L^{21})_2$	0-D/dimer	BOMCIQ	[61]
59	$[(nBu)_2Sn]_2(L^{27})_2$, CH_3CN	0-D/dimer	JOVQET	[64]
60	$[(nBu)_2Sn]_2(L^{28})_2$	0-D/dimer	JOVQIX	[64]
61	$[(nBu)_2Sn]_2(L^{29})_2$	0-D/dimer	JOVQOD	[64]
62	$[(nBu)_2Sn]_2(L^{30})_2$, $2(CHCl_3)$	0-D/dimer	JOVQUJ	[64]
63	$[(tBu)_2Sn]_2(L^{18})_2$, $4(C_4H_8O)$	0-D/dimer	DORZIT	[65]
64	$[(PhCH_2)_2Sn]_2(L^{31})_2$, CH_2Cl_2	0-D/dimer	TOHBUP	[66]
65	$(Ph_2Sn)_2(L^{21})_2$	0-D/dimer	BOMCUC	[61]
66	$(Ph_2Sn)_2(L^{32})_2$, $6(C_6H_6)$	0-D/dimer	SEWGIM	[67]
67	$(Me_2SnCl)_2(L^{1})$	0-D/dimer	UJAFUH	[68]
68	$(Me_2SnCl)_2(L^{33})$	0-D/dimer	SEWGEI	[67]
69	$(Me_2SnCl)_2(L^{34})$, $2(CHCl_3)$	0-D/dimer	DOSJAY	[69]
70	$[(nBu)_2SnCl]_2(L^{1})$	0-D/dimer	UJAGAO	[68]
71	$[(nBu)_2SnCl]_2(L^{32})$	0-D/dimer	POMPOY	[70]
72	$[(nBu)_2SnCl]_2(L^{34})$	0-D/dimer	DOSJEC	[69]
73	$[(nBu)_2SnCl]_2(L^{35})$	0-D/dimer	PUNDOU	[71]
74	$(Ph_2SnCl)_2(L^{2})$	0-D/dimer	QUJVUN	[72]
75	$(Ph_2SnCl)_2(L^{32})$	0-D/dimer	POMPUE	[70]
76	$(Ph_2SnCl)_2(L^{36})$	0-D/dimer	SANMOL	[73]
77	$[PhSn(Cl)CH_2Si(Me)_2C_6H_4C_6H_4Si(Me)_2CH_2Sn(Ph)Cl](L^{2})$, $2(C_4H_8O)$	0-D/dimer	KOKJIG	[74]
78	$[PhSn(I)CH_2Si(Me)_2C_6H_4C_6H_4Si(Me)_2CH_2Sn(Ph)I](L^{2})$, CH_2Cl_2	0-D/dimer	KOKJAY	[74]
79	$(Cy_3Sn)_2(L^{37})_2$	0-D/dimer	JUMWEW	[75]
80	$[(PhCH_2)_3Sn]_2(L^{32})$	0-D/dimer	POMQAL	[70]
81	$[(2\text{-}FC_6H_4CH_2)_3Sn]_2(L^{2})$	0-D/dimer	EXEQAZ	[76]
82	$[(2\text{-}ClC_6H_4CH_2)_3Sn]_2(L^{2})$	0-D/dimer	EXUSEV	[77]
83	$[(Me_2(Ph)CCH_2)_3Sn]_2(L^{2})$	0-D/dimer	BESKUG	[78]
84	$(Ph_3Sn)_2(L^{2})$, CH_2Cl_2	0-D/dimer	POFVAI	[79]
85	$(Ph_3Sn)_2(L^{2})$, $2(CH_3OH)$	0-D/dimer	MOTLUC	[80]
86	$(Ph_3Sn)_2(L^{2})$, $2(H_2O)$	0-D/dimer	NORSAP	[81]
87	$(Ph_3Sn)_2(L^{31})$	0-D/dimer	TOHGEE	[66]
88	$(Ph_3Sn)_2(L^{32})$	0-D/dimer	POMQEP	[70]
89	$(Ph_3Sn)_2(L^{33})$, $1.5(CHCl_3)$	0-D/dimer	YIGHAZ	[67]
90	$(Ph_3Sn)_2(L^{36})$	0-D/dimer	SANMIF	[73]
91	$(Me_2SnCl)_3(L^{38})$	0-D/trimer	UJAGES	[68]
92	$(Me_2SnCl)_3(L^{39})$	0-D/trimer	UJAGIW	[68]
93	$[(tBu)_2SnCl]_3(L^{38})$, CH_3CH_2OH	0-D/trimer	UJAGOC	[68]
94	$(Ph_2SnCl)_3(L^{38})$	0-D/trimer	NOLKUV	[82]
95	$(Ph_2Sn)_3(L^{39})_2$, $2(CHBr_3)$	0-D/trimer	NOLLEG	[82]
96	$(Ph_2Sn)_3(L^{40})_2$, $2(CHCl_3)$, $3(C_6H_6)$	0-D/trimer	NOLLAC	[82]
97	$\{(H_3O)[Ce(L^{2})_2]$, $2.5(CH_3NO_2)$, $1.5(H_2O)\}_n$	3-D	PAYPEN	[83]
98	$\{(H_3O)[Sm(L^{2})_2]$, $2.5(CH_3NO_2)$, $1.5(H_2O)\}_n$	3-D	PAYPIR	[83]
99	$\{(H_3O)[Eu(L^{2})_2]$, $2.5(CH_3NO_2)$, $1.5(H_2O)\}_n$	3-D	PAYPOX	[83]
100	$\{(H_3O)[Gd(L^{2})_2]$, $2.5(CH_3NO_2)$, $1.5(H_2O)\}_n$	3-D	PAYPUD	[83]
101	$\{(H_3O)[Tb(L^{2})_2]$, $2.5(CH_3NO_2)$, $1.5(H_2O)\}_n$	3-D	PAYQAK	[83]
102	$\{(H_3O)[Nd(L^{2})_2]$, $2.5(CH_3NO_2)$, $1.5(H_2O)\}_n$	3-D	XUPQUW	[84]

3. Results

3.1. Coordination Chemistry of a Molybdenum Poly-Dithiocarbamate Complex

In the crystal of **1** [29], originally prepared in connection with studies on steric effects exerted by ligands upon the electrochemistry and kinetics of oxygen atom transfer reactions of relevance to oxomolydenum(VI) enzymes such as sulphite oxidase, two $Mo(=O)_2$ centres

are bridged by two L^1 dianions to form a di-nuclear molecule, $[Mo(=O)_2(L^1)]_2$, as shown in Figure 2. The assembly lacks crystallographic symmetry, and the molybdenum(VI) centres exist in distorted octahedral coordination geometries defined by O_2S_4-donor sets, as the dithiocarbamate residues are chelating.

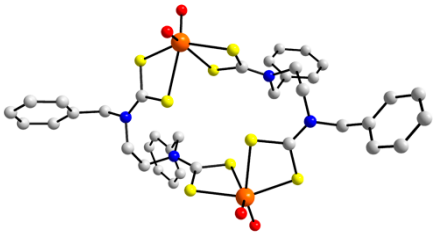

Figure 2. The di-nuclear molecule of $[Mo(=O)_2(L^1)]_2$ in the crystal of **1**. Colour code and protocols for this and subsequent diagrams: central metal atom, orange; sulphur, yellow; red, oxygen; blue, nitrogen; grey, carbon. Hydrogen atoms have been omitted for clarity.

3.2. Coordination Chemistry of Ruthenium Poly-Dithiocarbamate Complexes

There are two structures conforming to the general formula [Ru](S_2CN-spacer-NCS_2)[Ru]. Whereas the structure of di-cationic $\{[(dppm)_2Ru]_2(L^2)\}^{2+}$ in **2** [30] lacks crystallographic symmetry, that of neutral $[Cp(Ph_3P)Ru]_2(L^3)$ in **3** [31], Figure 3a, is disposed about a centre of inversion; dppm is $Ph_2PCH_2PPh_2$ and Cp is $C_5H_5^-$. The L^3 di-anion in **3** was synthesised by the insertion of phenylisothiocyanate into the silicon–sulphur bond of a silanethiolate precursor complex [31]. The coordination geometry for ruthenium in each case is based on a distorted octahedron. In the realisation of the synthetic target towards the formation of hetero-metallic systems, an unusual hetero-metallic species was characterised in **4** [32], namely $[(dppm)_2Ru(L^2)Pd(PPh_3)_2]^{2+}$. The di-cation was prepared from the reaction of $[Ru(S_2CNC_4H_8NH)(dppm)_2](BF_4)_2$ with carbon disulphide under basic conditions followed by the addition of $[PdCl_2(PPh_3)_2]$ [32]. In the structure, Figure 3b, the L^2 di-anion links ruthenium(II) and palladium(II) atoms by chelating each metal centre. The coordination geometry for the ruthenium(II) atom resembles that in **2**; the anticipated distorted square-planar geometry is seen for the palladium(II) atom.

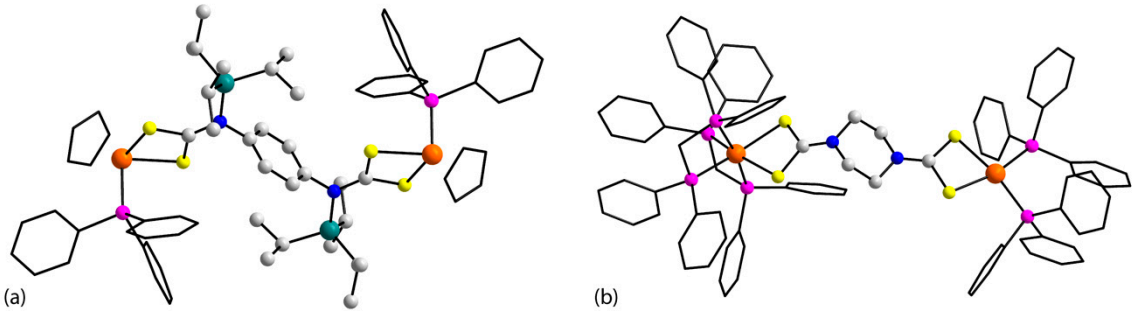

Figure 3. The di-nuclear molecules of (**a**) $\{[Cp(Ph_3P)Ru]_2(L^3)\}^{2+}$ in **3** and (**b**) $[(dppm)_2Ru(L^2)Pd(PPh_3)_2]^{2+}$ in **4**. Additional colour code: teal, silicon; pink, phosphorus. The carbon atoms of the Cp, Ph_3P, and dppm molecules are illustrated in stick mode.

3.3. Coordination Chemistry of Nickel-Triad Poly-Dithiocarbamate Complexes

Poly-nuclear dithiocarbamate complexes are known for each of the nickel-triad elements with those of palladium being structurally characterised the most frequently. Across the triad, regardless of the metal centre, only two distinct structural motifs are observed. There are three di-nuclear nickel(II) complexes formulated as di-cationic {[Ni](S_2CN-spacer-NCS_2)[Ni]}$^{2+}$, each of which is disposed about a centre of inversion. The di-cations found in the crystals of **5**–**7**, respectively, are $\{[(dppe)Ni]_2(L^2)\}^{2+}$, $\{[(dppf)Ni]_2(L^2)\}^{2+}$ [33], as illustrated in Figure 4a, and $\{[(dppf)Ni]_2(L^1)\}^{2+}$ [34]; dppe is $Ph_2P(CH_2)_2PPh_2$ and

dppf is $Ph_2P(C_5H_4FeC_5H_4)PPh_2$; these were prepared from the metathetical reactions of $NiCl_2$(dppe) or $NiCl_2$(dppf) with the potassium salts of L^1 or L^2, and they were used in the functionalisation of gold nanoparticles by the displacement of a citrate shell [33]. In each case, the P_2S_2 donor sets in each di-nuclear molecule define a distorted square-planar geometry. The second structural motif is also di-nuclear but charge-neutral and has been characterised in two crystals, namely $Ni_2(L^4)_2$ (**8**) [35], as shown in Figure 4b, and $Ni_2(L^5)_2$ (**9**) [36]. Here, the $-CS_2^-$ residues are well-separated and provide bridges to two nickel(II) atoms, each within a square-planar geometry defined by a S_4-donor set. In **8**, being an early example describing the use of dithiocarbamate ligands for the construction of metal-directed, self-assembled di-metallic cryptands, the di-nuclear molecule is disposed about a centre of inversion and has an open conformation. By contrast, there is no crystallographic symmetry imposed for the di-cation in **9**, which has a twisted conformation.

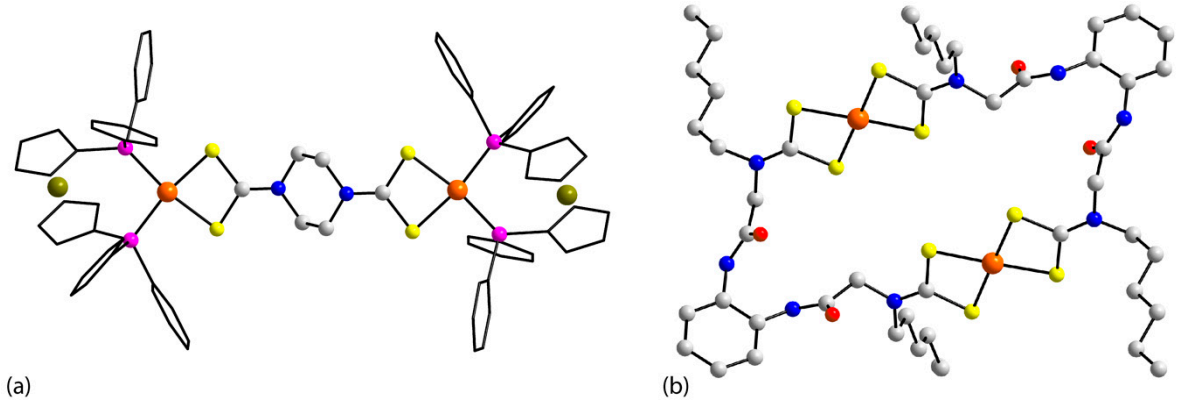

Figure 4. The di-nuclear molecules of (**a**) $\{[(dppf)Ni]_2(L^2)\}^{2+}$ in **6** and (**b**) $Ni_2(L^4)_2$ in **8**. Additional colour code: dark-yellow, iron. The carbon atoms of the dppf molecules are illustrated in stick mode.

The palladium structures in this section adopt the same structural motifs as for nickel(II). For the motif shown in Figure 4a, two polymorphic forms are known for the $\{[(Ph_3P)_2Pd]_2(L^2)\}^{2+}$ di-cation, one being disposed about a centre of inversion (**10**) and the other lacking symmetry (**11**) [37]; $\{[(Ph_3P)_2Pd]_2(L^1)\}^{2+}$ in **12** [37] also lacks symmetry. The primary motivation for the synthesis of **10**–**12** is related to the study of their potential catalytic activity [37], being evaluated as catalysts for the selective C–H bond functionalisation in the methoxylation of benzo[h]quinoline: the obtained yields of 10-methoxybenzo[h]quinoline were high for each putative catalyst [37]. The same structural motif shown in Figure 4a is found in each of $\{[(dppf)Pd]_2(L^1)\}^{2+}$ (**13**) [34] and $\{[(dppf)Pd]_2(L^2)\}^{2+}$ (**14**) [33]. The structure of each of the next four palladium(II) complexes to be described adopts the di-nuclear structural motif illustrated in Figure 4b. Thus, $Pd_2(L^6)_2$ (**15**) [38] is centrosymmetric as for **8**. When the same molecule was isolated as its chloroform mono-solvate, in **16** [38], it lacks the crystallographic symmetry of **15**, but it adopts essentially the same conformation. The molecular structure of $Pd_2(L^5)_2$ (**17**) [36] closely resembles that of the nickel(II) analogue, $Ni_2(L^5)_2$ (**9**) [36] and was prepared in a one-pot synthesis from the diamine, carbon disulphide, potassium hydroxide with K_2PdCl_4 in THF-H_2O. A rather more complicated dithiocarbamate di-anion, that is, L^7, being constructed about a dihydroxycalix(4)arene residue, is noted in the crystal of **18**, leading to a di-nuclear complex formulated as $Pd_2(L^7)_2$ [39]. Despite the complexity of the formula, the centrosymmetric, di-nuclear molecule resembles the simpler analogues described above.

There are only two platinum(II) complexes with poly-functional dithiocarbamate di-anions, namely, di-cationic and centrosymmetric $\{[(Et_3P)_2Pt]_2(L^2)\}^{2+}$ (**19**) and $\{[(Ph_3P)_2Pt]_2(L^2)\}^{2+}$ (**20**) [33], which resemble closely their nickel and palladium congeners.

3.4. Coordination Chemistry of Copper and Gold Poly-Dithiocarbamate Compounds

A total of 18 structures fall into this category, and a fascinating variety of structural motifs are observed for the seven copper-containing and 11 gold-containing structures, there being no examples of silver-containing species. The structural diversity notwithstanding, all aggregation patterns lead to zero-dimensional species.

Five of the copper complexes are di-nuclear and contain copper in varying oxidation states. Two copper(I) centres are linked by a μ_2-bridging L^2 di-anion in $[(Ph_3P)_2Cu]_2(L^2)$ (**21**) [40], prepared from the reaction of $(Ph_3P)_2Cu(NO_3)$ and $Na_2(L^2)$, and these were of interest for their molecular conducting and non-linear optical properties. The centrosymmetric molecule in **21**, shown in Figure 5a, with a P_2S_2-donor set defining a distorted tetrahedral geometry, is also seen in $[(Ph_2PCH_2N(Ph)CH_2PPh_2)Cu]_2(L^2)$ (**22**) [41], having a less commonly observed diphosphane ligand and synthesised for an investigation of its photophysical properties. The next three structures feature well-spaced dithiocarbamate residues enabling the chelation of two copper centres and the formation of metal-containing macrocycles. In the centrosymmetric di-cation, $\{[Cu_2(L^8)_2]\}^{2+}$, of crystal **23** [42], the square-planar copper centres are in the +III oxidation state, providing an exemplary example of the ability of the dithiocarbamate ligand being able to stabilise high oxidation states owing to a significant contribution of the dithiolate canonical form, that is, $(^-S)_2C{=}N^+R_2$, to the electronic structure of the dithiocarbamate residue. Indeed, the motivation for the synthesis of **23** is related to investigations of electrochemical anion sensing by copper-based, redox-active, self-assembled macrocycles. A similar molecular structure is found in neutral $Cu_2(L^9)_2$ (**24**) [43], Figure 5b, indicating the presence of copper(II) centres. A more complicated situation occurs in the crystal of mixed-valent **25** [44], which is the product of the oxidation of **24** and features large aromatic spacer groups enabling the control of cavity size in the resultant aggregates. The complex is formulated as the catenane, $\{[Cu_2(L^9)_2]\}_2^{2+}$, and lacks crystallographically imposed symmetry; each di-nuclear molecule contains both copper(II) and copper(III) centres. One component of the catenane is shown in Figure 5c, and the mutual interpenetration of two molecules leading to the catenane is represented in Figure 5d.

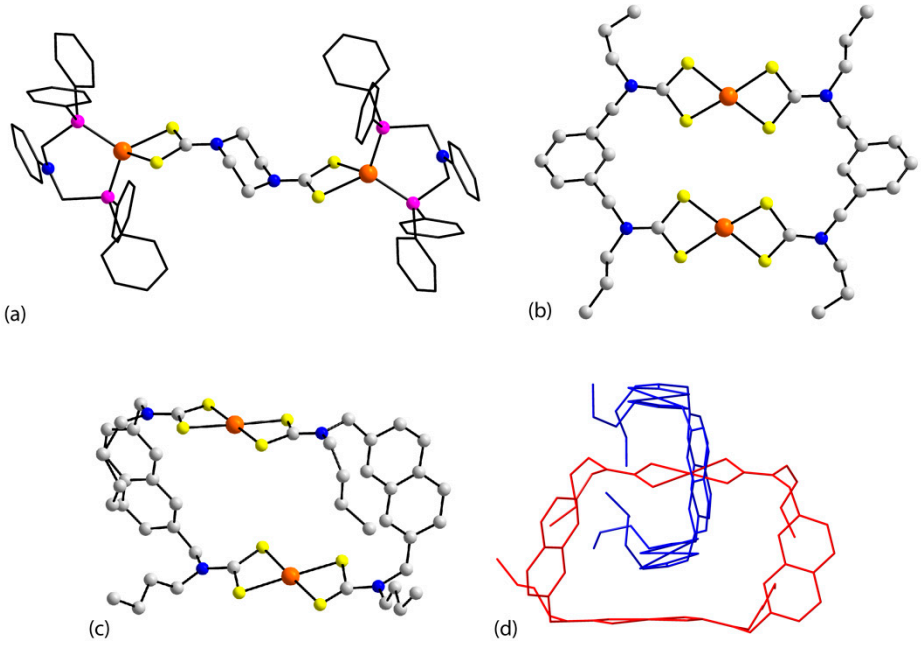

Figure 5. The di-nuclear molecules of (**a**) $[(Ph_2PCH_2N(Ph)CH_2PPh_2)Cu]_2(L^2)$ in **22**, (**b**) $Cu_2(L^9)_2$ in **24** and (**c**) $[Cu_2(L^9)_2]^+$ in **25**. (**d**) The catenane, $\{[Cu_2(L^9)_2]\}_2^{2+}$, in **25** in stick form. The carbon atoms of the $Ph_2PCH_2N(Ph)CH_2PPh_2$ molecules are illustrated in stick mode.

When the dithiocarbamate di-anion L^{10} complexes copper(I) centres, a tetra-nuclear aggregate is observed, namely $Cu_4(L^{10})_2$ (**26**) [43]. As seen from Figure 6a, each μ_3-bridging dithiocarbamate residue links three copper(I) centres whereby one sulphur atom connects to one copper(I) atom and the second sulphur atom connects to two copper(II) atoms. The core of the cluster is a distorted Cu_4 tetrahedron disposed about a 2-fold axis of symmetry. The final copper structure to be described reverts to square-planar copper(III) centres in octa-nuclear $[Cu_8(L^{11})_4]^{8+}$ of (**27**), which were developed for host–guest chemistry [45]. The octa-cationic species has S_4 symmetry and features four resorcarene ligands, each functionalised with four dithiocarbamate residues, with each residue chelating a copper(III) centre, as detailed in Figure 6b. Four such resorcarene ligands are connected into a tetrahedral assembly, being mediated by the eight copper(III) atoms, resulting in the cluster shown in Figure 6c.

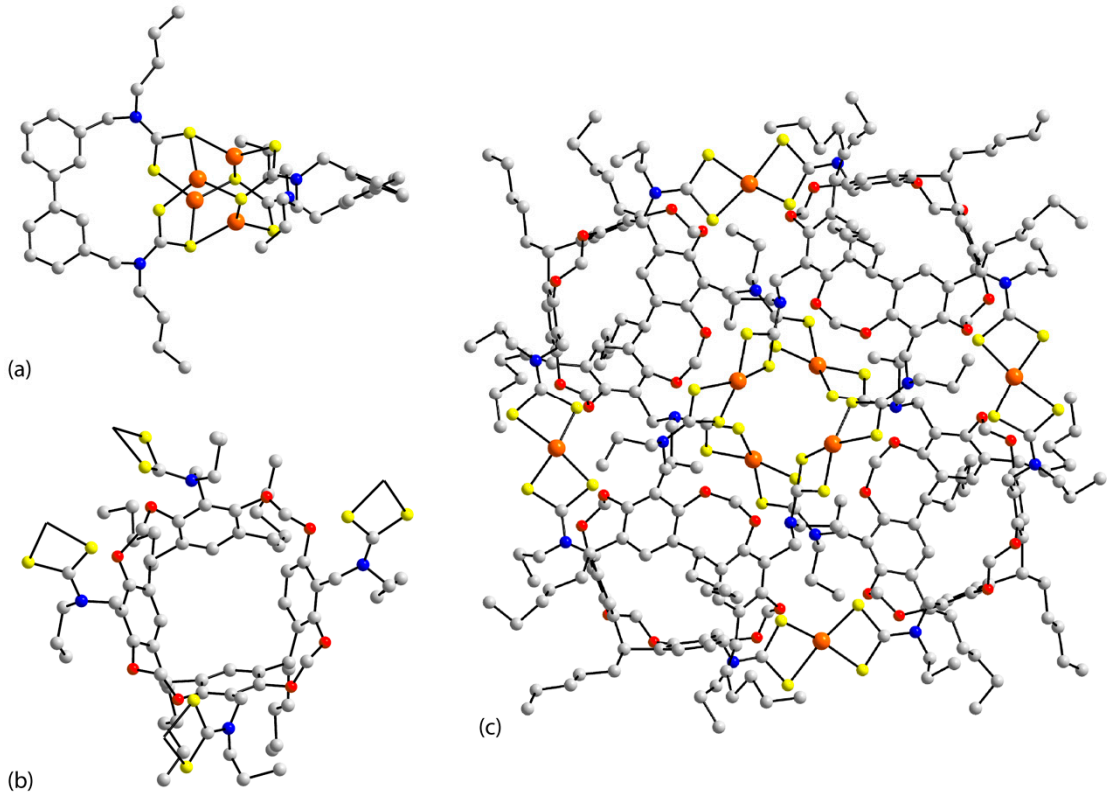

Figure 6. (**a**) Molecular structure of tetra-nuclear $Cu_2(L^{10})_2$ in **26**, (**b**) detail of the tetradentate mode of coordination of the L^{11} di-anion in $[Cu_8(L^{11})_4]^{8+}$ in **27** and (**c**) molecular structure of octa-nuclear $[Cu_8(L^{11})_4]^{8+}$ in **27**.

Of the 11 gold complexes of poly-functional dithiocarbamate ligands, three are di-nuclear, and of these, two are gold(I) mono-phosphane species, $(Me_3PAu)_2(L^1)$ in the crystal of **28** [34], Figure 7a, and $(Ph_3PAu)_2(L^1)$ in **29** [34]; these were prepared by the facile reaction of the phosphanegold(I) chloride precursor with $K_2(L^1)$. Each of these molecules is situated about a centre of inversion, and a monodentate mode of coordination is noted for the dithiocarbamate residue. While the crystallographic symmetry persists in the molecule of $[(Ph_3P)_2Au]_2(L^2)$ in **30** [46], as shown in Figure 7b, which was prepared as a synthetic precursor for gold nanoparticles, a distinct coordination geometry is apparent arising from a different mode of coordination by the dithiocarbamate residue. Thus, the gold atom is coordinated by two phosphane-P atoms and is simultaneously chelated by the dithiocarbamate residue, albeit with significantly longer Au–P and Au–S bond lengths compared to those observed in **28** and **29**; the P_2S_2-donor set in **30** defines a distorted tetrahedral geometry, resembling the nickel(II) and copper(I) congeners, for example **6** and **22**, illustrated in Figures 4a and 5a, respectively. Each of the independent

dithiocarbamate residues in the $\{[(dppf)Au_2]_2(L^2)\}^{2+}$ di-cation of **31** [47], prepared by the reaction of $(dppf)(AuCl)_2$, $K_2(L^2)$ and $NH_4[PF_6]$, employs each sulphur atom in a bond to a gold atom. These are further bridged by a dppf molecule to form the tetra-nuclear molecule illustrated in Figure 7c. This arrangement facilitates the formation of aurophilic (Au ··· Au) bonds, which are long known to be prevalent in the supramolecular chemistry of gold complexes [85–87]. Such aurophilic interactions also feature prominently in the subsequent multi-nuclear structures to be described in this section.

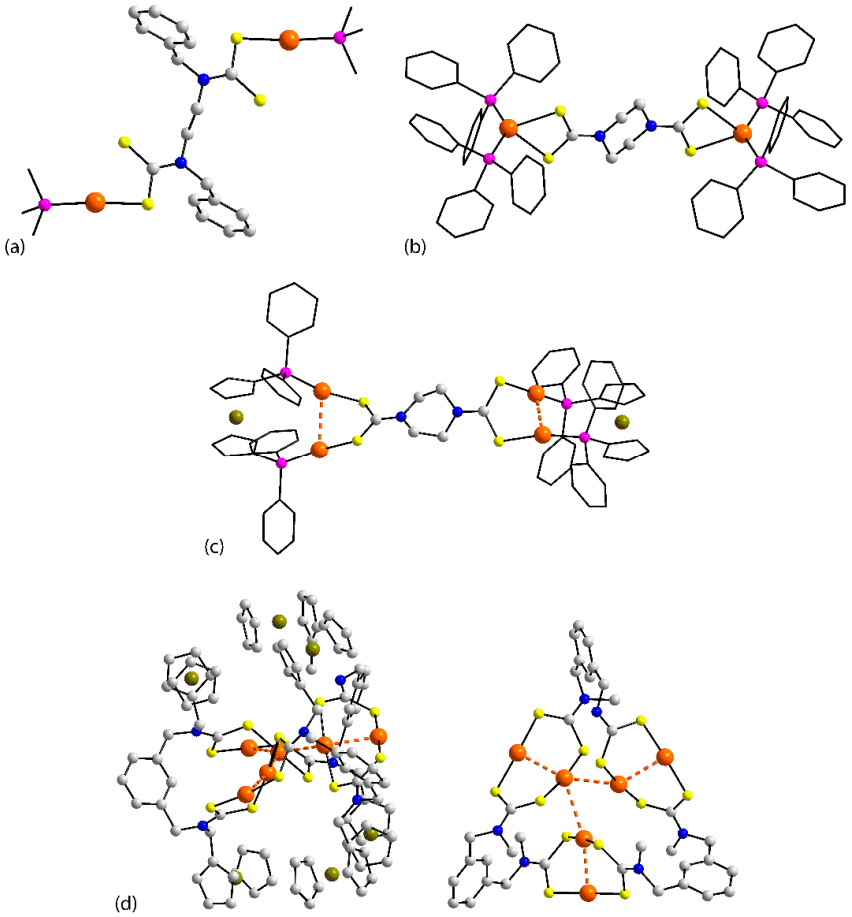

Figure 7. Molecular structures of (**a**) di-nuclear $(Me_3PAu)_2(L^1)$ in the crystal of **28**, (**b**) di-nuclear $[(Ph_3P)_2Au]_2(L^2)$ in **30**, (**c**) tetra-nuclear $[(dppf)Au_2]_2(L^2)$ in **31**, and (**d**) hexa-nuclear $Au_6(L^{12})_3$ in **32**, with a simplified version shown in the right-hand side image. When present, the orange dashed lines represent aurophilic (Au ··· Au) bonding interactions.

A hexa-nuclear aggregate, $Au_6(L^{12})_3$, is evident in the crystal of **32** [48] and is represented in the two views of Figure 7d. As in **31**, each sulphur atom of each dithiocarbamate residue links a gold atom so that each L^{12} di-anion connects to four gold atoms, and in turn, each gold atom is linked to two L^{12} di-anions; the aggregate lacks symmetry. This arrangement leads to the formation of three eight-membered {SCSAu ··· AuSCS} rings, each encompassing an aurophilic interaction. In addition, there are two inter-dimer aurophilic interactions contributing to the stability of the hexamer, and this arrangement facilitates a close to co-planar arrangement of the six gold atoms. The remaining structures contain even more gold atoms in the assembled zero-dimensional aggregates. The motivation for their synthesis was multi-faceted with the primary idea to generate, via a stepwise macro-cyclisation strategy exploiting aurophilic interactions, giant ring systems with potential applications in host–guest chemistry, molecular recognition, and possibly as selective luminescent materials for sensors and OLEDs.

The structures of **33** and **34** [49] have the common feature of having neutral species formulated as $Au_8(L^{13})_2$. The L^{13} tetra-anion, a tetrakis-dithiocarbamate-calix[4]arene ligand, employs each of the eight sulphur atoms to connect a distinct gold atom. Each of the latter is connected similarly to a second L^{13} tetra-anion to generate an octa-nuclear capsule or, alternatively, a "gold(I)-containing metallosupramolecular cage"; the aggregate lacks symmetry. Each gold atom is linearly coordinated within an S_2-donor set. The capping of pairs of gold atoms results is the formation of four eight-membered {SCSAu ··· AuSCS} rings featuring intramolecular aurophilic interactions, as seen in Figure 8a. There are additional, weaker aurophilic interactions within the cage as well as intermolecular aurophilic interactions; the latter lead to a supramolecular layer in the crystal. Similar "quadruple-stranded helicate dimeric cages" are found for the two independent molecules comprising the asymmetric unit of **34**; however, a difference occurs in that the intermolecular aurophilic interactions evident in **33** are absent in the crystal of **34**. A similar mode of coordination to that just described is observed for the six L^{14} ligands in the neutral molecule of $Au_{12}(L^{14})_6$ in the crystal of **35** [50]; the aggregate lacks symmetry, as shown in Figure 8b. The connections between the 12 gold(I) atoms lying in an approximate plane are mediated by aurophilic interactions and the bridging dithiocarbamate residues resides alternatively above and below the best plane through the Au_{12} ring.

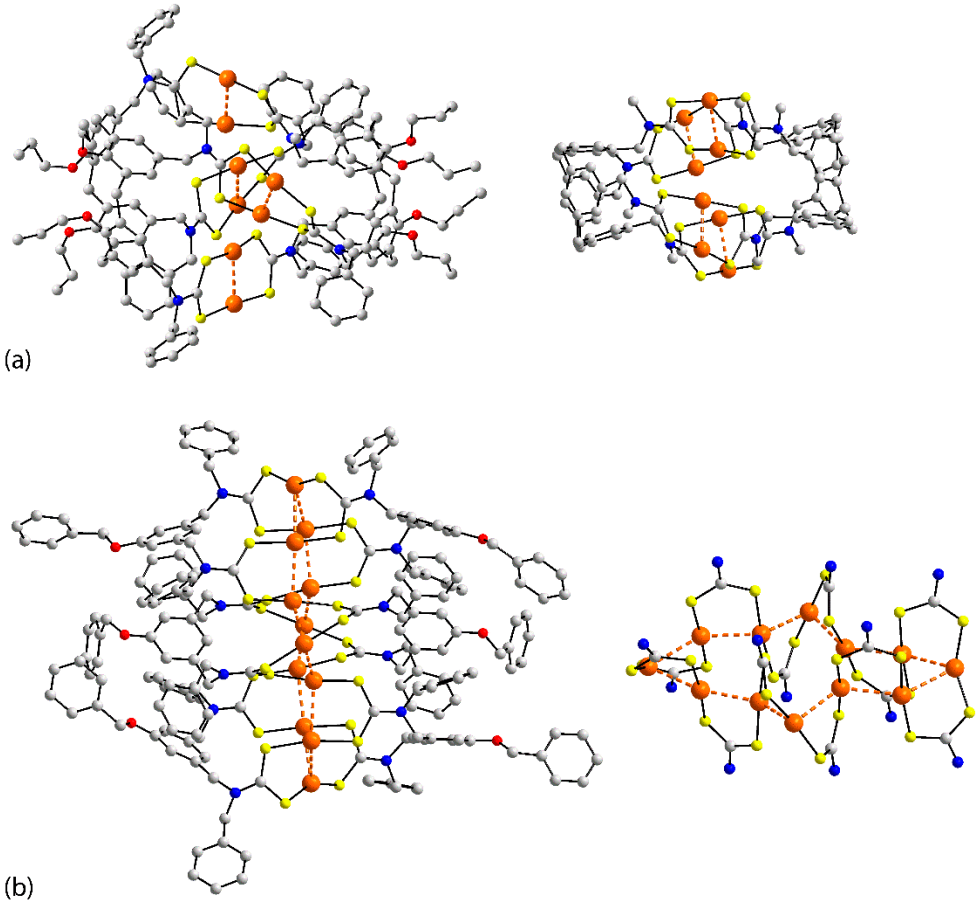

Figure 8. Molecular structures of (**a**) octa-nuclear $Au_8(L^{13})_2$ in the crystal of **33** and (**b**) dodeca-nuclear $[Au_{12}(L^{14})_6]$ in **35**, with simplified versions shown on the right-hand side of each image.

The basic repeating unit in the 16-gold atom cluster, octa-cationic $[Au_{16}(L^{15})_4]^{8+}$, in the crystal of **36** [51] is a tetramer, that is, di-cationic $\{[(dppm)Au_2]_2(L^{15})\}^{2+}$, whereby each sulphur atom of each dithiocarbamate residue binds a gold atom. The pairs of gold atoms linked by each dithiocarbamate residue are also bridged by a dppm ligand, leading to eight-membered {–PCPAuSCSAu} rings. As observed above, when this mode of coordination is

apparent, intramolecular aurophilic interactions are formed. In addition, six intermolecular aurophilic interactions are apparent, leading to two curved chains comprising eight gold atoms each, as shown in Figure 9a. A 16-membered gold atom ring is not formed as the separation between two pairs of terminal gold atoms, of approximately 4.40 Å, is considered too long to represent a significant interaction between the atoms. The dithiocarbamate residues around the ring lie on opposite sides, as highlighted in the simplified view of Figure 9a. A similar molecular structure is found in the crystal of **37**, featuring $[Au_{16}(L^2)_4]^{8+}$ octa-cations [52], as shown in Figure 9b. The mode of coordination of the L^2 di-anions and their alternating sequence of orientations around the girth of the molecule are as for **36**. A difference occurs as in this case; there are aurophilic interactions between each adjacent pair of gold atoms, so the 16 gold atoms define a closed ring with the shape of a bowl, as shown in Figure 9b.

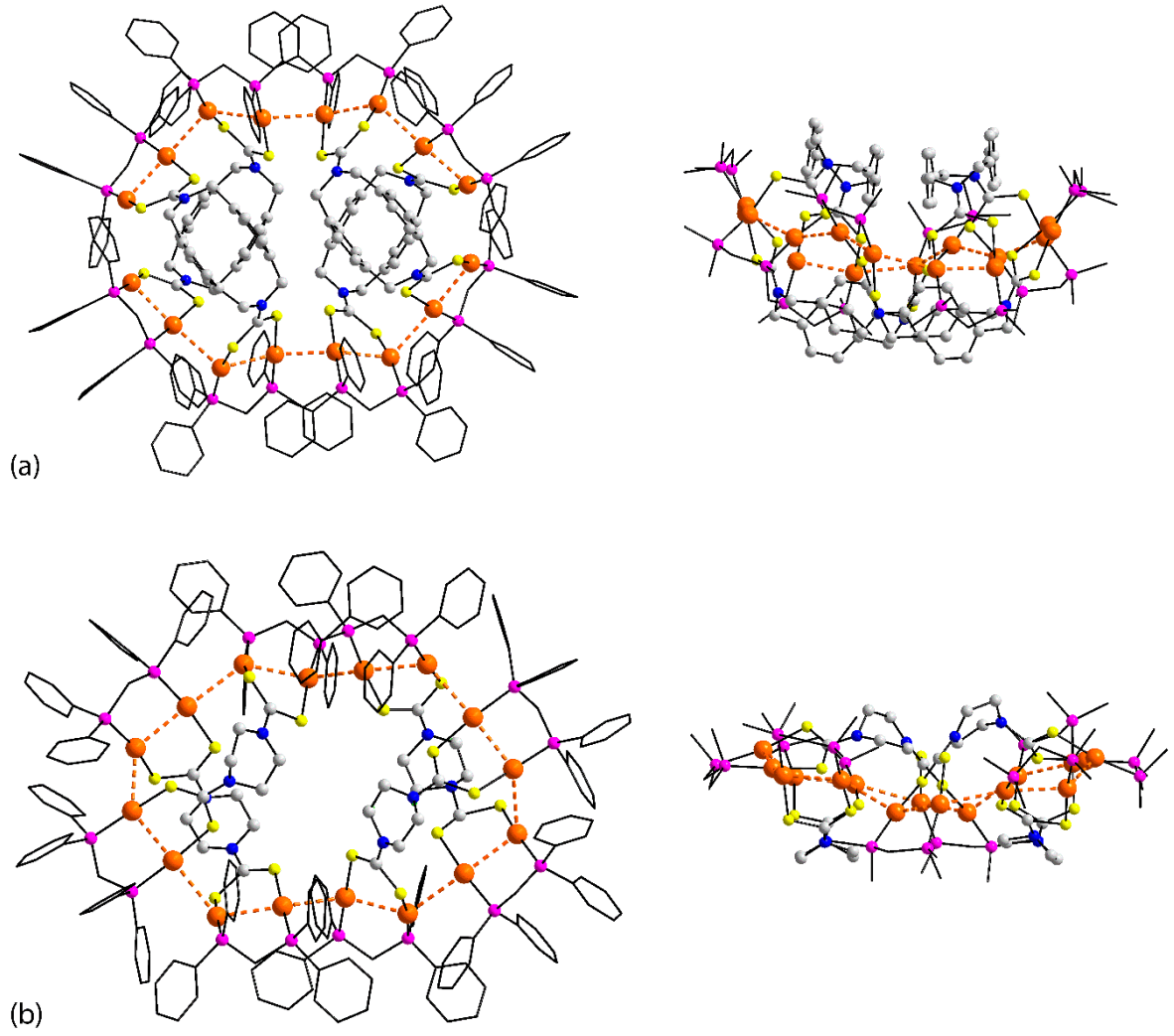

Figure 9. Molecular structures of (**a**) $[Au_{16}(L^{15})_4]^{8+}$ in the crystal of **36** and (**b**) $[Au_{16}(L^2)_4]^{8+}$ in **37**, with simplified versions shown on the right-hand side.

The final structure to be described in this section is that of **38**, $Au_{36}(L^{12})_{18}$ [48], which is notable for being a 36 gold atom cluster, as shown in Figure 10. The simplest description of the molecule revolves around a 24-membered ring comprising gold atoms, each forming an aurophilic interaction with its neighbour. Decorating the ring are six additional pairs of gold atoms connected every four Au ··· Au bonds along the circumference of the ring and orientated perpendicular to the ring so one of the gold atoms is linked to the ring by a pair of aurophilic interactions leading to a {··· Au ··· Au ··· Au} triangle. This can be seen

in the lower views of Figure 10, where the L^{12} dithiocarbamate ligands have been colour-coded to emphasise the $Au_6(L^{12})_3$ repeat unit, which resembles a first approximation of the molecular structure observed for the hexa-nuclear $Au_6(L^{12})_3$ cluster in the crystal of **32**, as shown in Figure 7d.

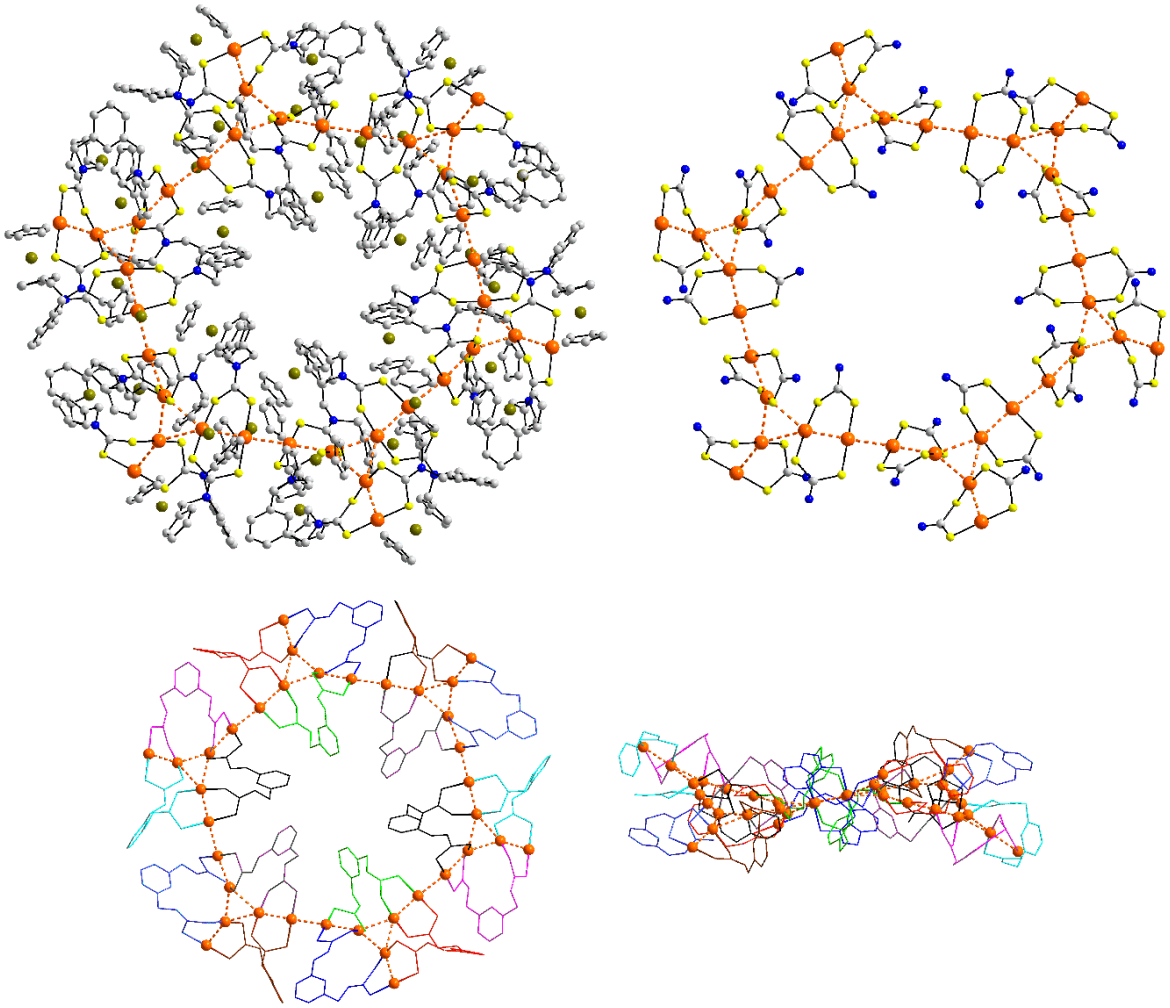

Figure 10. Views of the molecular structure of $[Au_{36}(L^{12})_{18}]^{8+}$ in the crystal of **38** and simplified versions. In the lower views, each L^{12} di-anion has been colour-coded.

3.5. Coordination Chemistry of Zinc-Triad Poly-Dithiocarbamate Compounds

The most numerous examples in this section are species containing zinc with smaller numbers of examples containing cadmium and mercury. There are four instances of di-nuclear zinc(II) aggregates and, curiously, each presents a distinct structural motif, as shown in Figure 11. The original interest in **39** [53] and **40** [54], examples of ditopic poly-ferrocenyl zinc(II)-dithiocarbamate macrocyclic receptors, was to investigate the ability of these substrates to bind and sense, electrochemically, anionic guest species such as isonicotinate and benzoate. Both species were prepared via an in situ route; for example, **39** was prepared from the one-pot reaction of the relevant diamine ligand, potassium hydroxide, carbon disulphide, and zinc(II) acetate hydrate. In the di-nuclear $Zn_2(L^{16})_2$ molecule in the crystal of **39** [53], the dithiocarbamate residues of di-anionic L^{16} coordinate in a distinctive fashion, with one chelating one zinc(II) centre and the other residue being bidentate, μ_2-bridging. In this way, an eight-membered $\{–ZnSCS\}_2$ ring is formed and, being disposed about a centre of inversion, it has an extended chair conformation, as shown in Figure 11a; transannular Zn ··· S contacts are noted. The remaining examples, namely $Zn_2(L^{12})_2$ in the crystal of **40** [54], $Zn_2(L^5)_2(pyridine)_2$ in **41** [36], and $Zn_2(L^9)_2(N(CH_2CH_2)_3N)$ in **42** [55] each have the

common feature that both dithiocarbamate residues are chelating. As shown in Figure 11b, the two zinc(II) centres in **40** are well separated from each other; two independent, non-symmetric molecules comprise the asymmetric unit. The shared feature of the zinc(II) coordination geometries in **39** and **40**, each defined by an S_4-donor set, is the adoption of distorted tetrahedra. The structural chemistry of mono-functional dithiocarbamate compounds of the zinc-triad elements has been reviewed recently [13], and both dimeric and monomeric structural precedents for each of **39** and **40** are known, but there is a definite predominance of the dimeric form [13]. Isolated monomeric species are generally adopted when the pendant R substituents are large such as in the case when R = cyclohexyl (Cy), as in $Zn(S_2CNCy_2)_2$ [88], pointing to an influence of steric hindrance upon the adoption of the structural motif adopted in the condensed phase. In the present circumstances, it is noted that there are 14 atoms in the S ··· S bridge between zinc(II) centres in **39** as opposed to 11 atoms in **40**, perhaps suggesting a greater number of atoms offer flexibility in the ligand backbone to enable dimerisation. Similar di-nuclear molecules to that observed in **40** form the core of the structures of **41** [36] and **42** [55] in which complexation to additional donors leads to new structural motifs.

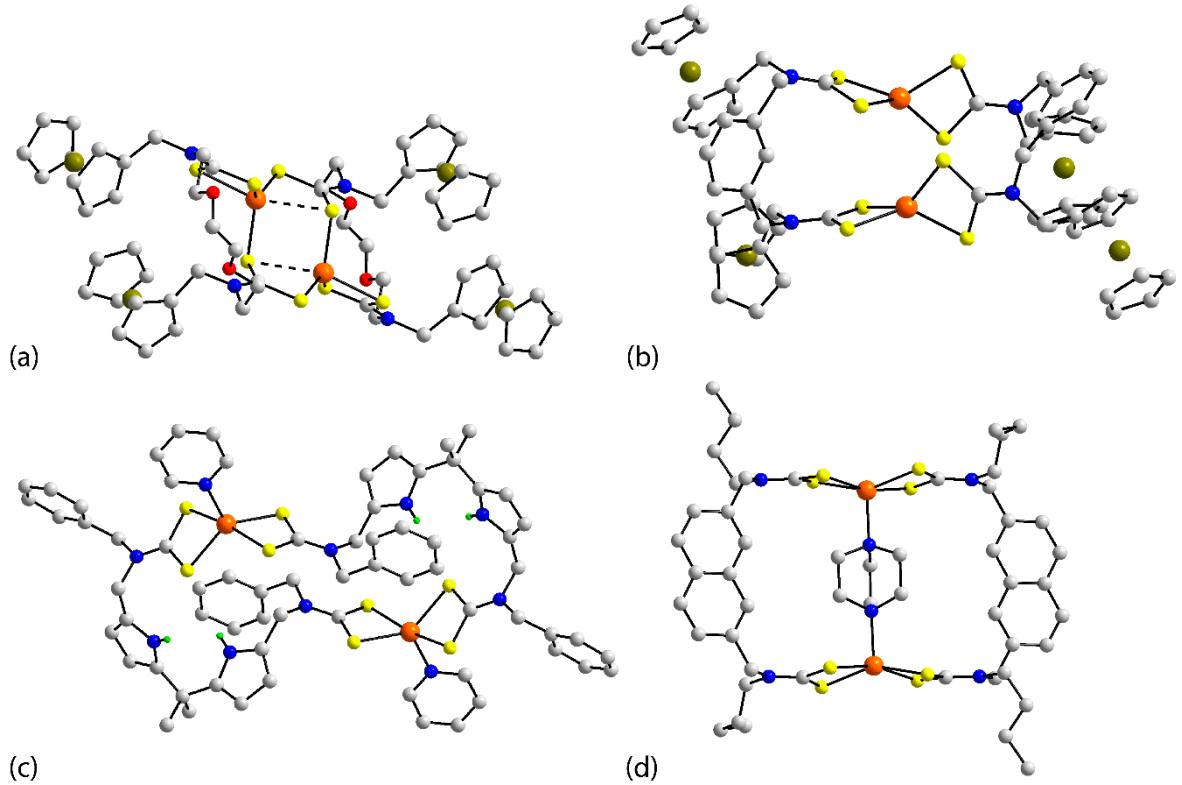

Figure 11. Molecular structures of (**a**) $Zn_2(L^{16})_2$ in the crystal of **39** (dashed lines indicate transannular Zn ··· S interactions), (**b**) $Zn_2(L^{12})_2$ in **40**, (**c**) $Zn_2(L^5)_2(pyridine)_2$ in **41** and (**d**) $Zn_2(L^9)_2(N(CH_2CH_2)_3N)$ in **42**. Additional colour code: green, for acidic hydrogen atoms.

In centrosymmetric **41** [36], each zinc(II) atom is additionally coordinated by a pyridine-nitrogen atom with the resulting NS_4-donor set being intermediate between distorted trigonal-bipyramidal and square-pyramidal, as shown in Figure 11c. In a sense, an inverse situation is evident in **42**, whereby a DABCO (1,4-diazabicyclo(2.2.2)octane) molecule provides an internal bridge between the two zinc(II) centres, so the dithiocarbamate-based macrocycle might be considered a receptor, as shown in Figure 11d. Here, the NS_4-donor set defines a coordination geometry approximating a square-pyramid; the di-nuclear molecule is disposed about a centre of inversion, implying the DABCO molecule is disordered. The coordination of the zinc-triad elements by additional donor atoms, such as pyridyl-nitrogen atoms, leads to a very rich diversity of structural outcomes [14], suggesting that further

work in this area is certainly warranted. The next two structures to be discussed are hexa-nuclear and, as for **40**–**42**, feature isolated zinc(II) centres as opposed to the dimers of **39**.

The tetrakis dithiocarbamate ligand based on four resorcarene ligands, L^{11}, in neutral $Zn_6(L^{11})_3$ in **43** [45] was observed previously in the $[Cu_8(L^{11})_4]^{8+}$ octa-cation of **27**, as shown in Figure 6c. However, in **43**, a different arrangement in the hexa-nuclear cluster is noted. Each dithiocarbamate ligand of L^{11} chelates a zinc atom, and these in turn connect to a second L^{11} tetra-anion in a cyclic fashion to form the ring shown in the images of Figure 12. The molecule has the shape of a cylinder and is disposed about a crystallographic site of symmetry $\bar{3}$. The NS_4-donor set for the independent zinc(II) atom is completed by a pyridine–nitrogen atom and defines a close to square-pyramidal geometry. The structure of $Zn_6(L^{17})_3$ in the crystal of **44** has also been described, where L^{17} is the N-bound n-butyl analogue of L^{11} [56]. There is an isomorphous relationship between **43** and **44**.

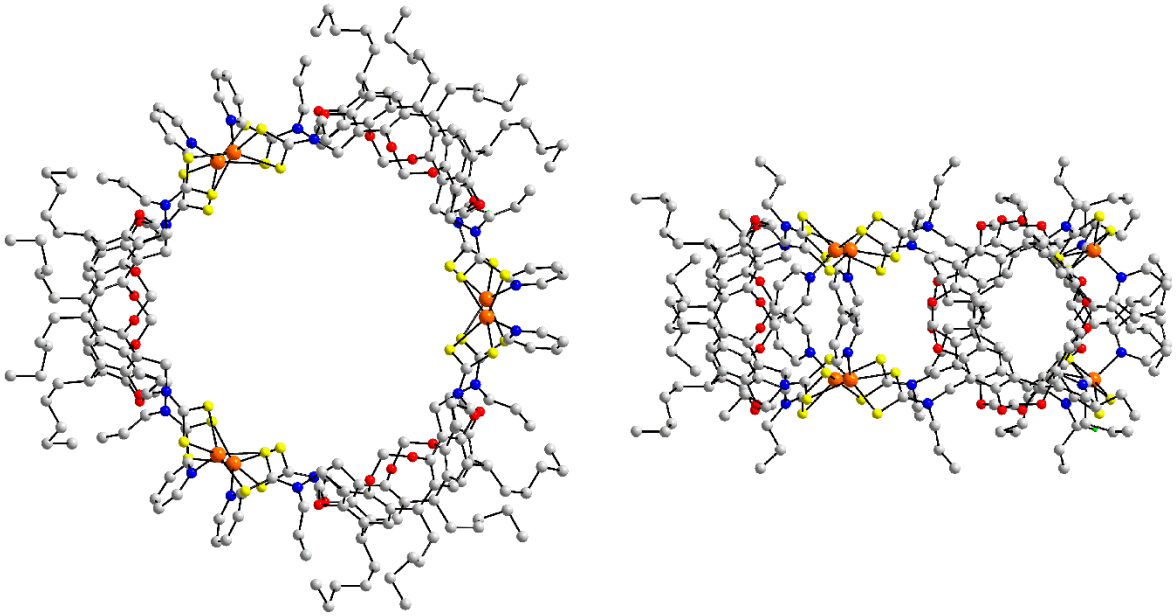

Figure 12. Molecular structure of neutral $Zn_6(L^{11})_3$ in the crystal of **43**: plan and side-on views.

The only coordination polymer is this section, which has only very recently been described, is formed in the crystal of **45**, comprising $[Zn(L^{18})]_n$ [57]. The structure is notable for two additional reasons. Firstly, it is the first of two rare examples in the present survey where the dithiocarbamate–nitrogen atom bears a proton and secondly, this compound is long known as an effective fungicide, marketed under the name Zineb® [89]. Indeed, **45** was one of the first industrially relevant fungicides, being commercially available as a fungicide for major crops in Europe and the United States of America during the second half of the 20th century. The asymmetric unit of **45** comprises a zinc(II) atom and two half L^{18} di-anions, each being disposed about a centre of inversion. The mode of coordination of one of the L^{18} di-anions is chelating, and that of the other is μ_2-bridging, resembling that seen in $[Zn_2(L^{16})_2]$ in **39**, as shown in Figure 11a. The result is illustrated in Figure 13, namely, a flat, two-dimensional coordination polymer. The thio–amide–N–H atoms project to either side of the layer, enabling the formation of N–H $\cdots$ S hydrogen bonds, leading to a three-dimensional architecture.

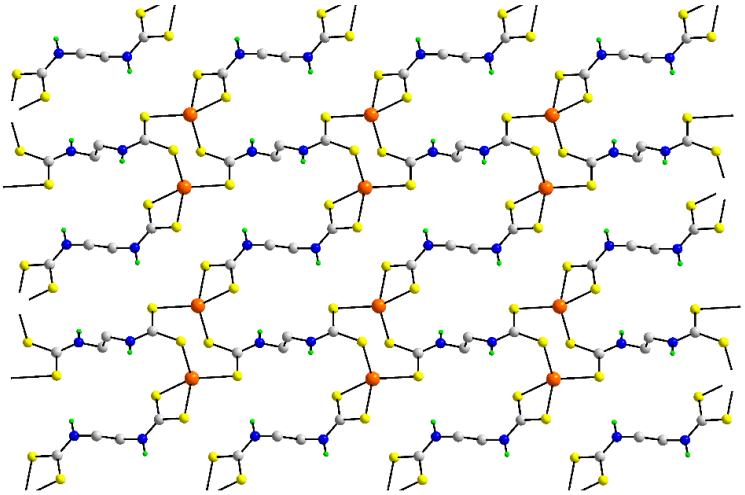

Figure 13. A plan view of the flat, supramolecular layer formed by $[Zn(L^{18})]_n$ in the crystal of **45**.

There are only two cadmium(II) structures to be described—that is, $Cd_6(L^{11})_3$ in **46** and $Cd_6(L^{17})_3$ in **47** [56], and these are isostructural with their zinc(II) analogues, **44** and **45**, with the hexa-nuclear molecule of the former illustrated in Figure 12. In each case, the NS_4-donor set defines square-pyramidal coordination geometry for the cadmium atom.

The first two of three mercury(II) dithiocarbamate structures to be described in this section are hitherto rare organometallic species. In $(PhHg)_2(L^{12})$ in crystal **48** [58], as shown in Figure 14a, each dithiocarbamate residue coordinates a mercury(II) atom in a monodentate mode, leading to a di-nuclear molecule; no intramolecular Hg ··· Hg interaction is apparent with the separation being 4.53 Å. Being a heterometallic compound containing both phenylmercury(II) residues and L^{12}, bearing ferrocenyl groups, the objective leading to the synthesis of **48** was to observe differences in the electrochemical and optoelectronic properties with the view of developing novel sensors [58]. Whereas in **48**, the phenylmercury species are proximate, occupying *syn* positions in the molecule, in centrosymmetric **49** [59], the phenylmercury components of $(PhHg)_2(L^{19})$ are *anti*, as shown in Figure 14b. Along with solvent, as detailed in Table 1, two independent molecules of $Hg_2(L^{20})_2$ comprise the asymmetric unit of **50** [60]; each of the latter is situated about a centre of inversion. One of the di-nuclear molecules is shown in Figure 14c from which it can be seen that one dithiocarbamate residue is chelating while the other is μ_2-bridging, leading to distorted tetrahedra defined by S_4-donor sets. This is the common structural motif adopted by mercury(II) mono-functional dithiocarbamate compounds [90].

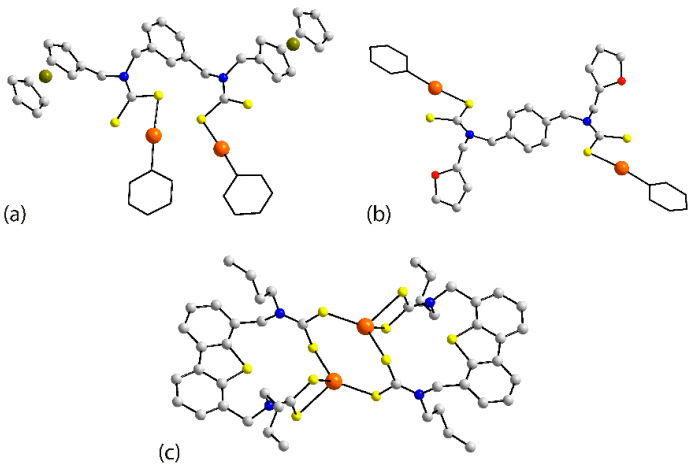

Figure 14. Molecular structures of (**a**) $(PhHg)_2(L^{12})$ in the crystal of **48**, (**b**) $(PhHg)_2(L^{19})$ in **49** and (**c**) $Hg_2(L^{20})_2$ in **50**.

3.6. Coordination Chemistry of Organotin Poly-Dithiocarbamate Compounds

Of all the elements included in this bibliographic review, the most represented are those of tin, with 46 examples. As highlighted in places below, much of the interest in the chemistry of tin dithiocarbamates lies with their various applications [91]. Despite the large number of structures, the number of structural motifs is rather small, being limited to five distinct aggregation patterns. In the following di-functional dithiocarbamate ligands are described before tri-functional analogues, within each category, diorganotin derivatives before triorganotin species, and the discussion is in order of increasing nuclearity of resultant zero-dimensional aggregate.

A total of 16 structures conform to the general formula $(R_2Sn)_2(S_2CN\text{-spacer-}NCS_2)_2$, namely $(Me_2Sn)_2(L^{21})_2$ in the crystal of **51** [61], $(Me_2Sn)_2(L^{22})_2$ (**52**) [61], $(Me_2Sn)_2(L^{23})_2$ (**53**) [61], $(Me_2Sn)_2(L^{24})_2$ (**54**) [62], $(Me_2Sn)_2(L^{25})_2$ (**55**) [63], $(Me_2Sn)_2(L^{26})_2$ (**56**) [61], $[(nBu)_2Sn]_2(L^{25})_2$ (**57**) [63], $[(nBu)_2Sn]_2(L^{21})_2$ (**58**) [61], $[(nBu)_2Sn]_2(L^{27})_2$ (**59**) [64], $[(nBu)_2Sn]_2(L^{28})_2$ (**60**) [64], $[(nBu)_2Sn]_2(L^{29})_2$ (**61**) [64], $[(nBu)_2Sn]_2(L^{30})_2$ (**62**), [64], $[(tBu)_2Sn]_2(L^{18})_2$ (**63**) [65], $[(PhCH_2)_2Sn]_2(L^{31})_2$, (**64**) [66], $(Ph_2Sn)_2(L^{21})_2$ (**65**) [61], and $(Ph_2Sn)_2(L^{32})_2$ (**66**) [67]. The original interest in compounds **51**, **52**, and, indeed, many of the other oligomeric compounds whose structures will be described herein, related to the desire to incorporate organotin groups, as representatives of organometallic compounds, into metallo-supramolecular architectures having cage-like, macrocyclic, or polymeric structures and having accessible sites for post-synthetic modification for the optimisation of molecular properties. As with many of the compounds in this overview, the synthesis was facile such as in the metathetical reaction leading to **51**: the diorganotin dichloride was reacted with $K_2[L^{21}]$. Additional interest in **59**–**61** related to their putative anti-cancer potential along with utility as precursors for the deposition of tin sulphide nanomaterials [64], each being classical applications of organotin dithiocarbamates [91]. The screening for anti-cancer potential indicated that the halogen-containing substituents in the dithiocarbamate ligands, as in **59** and **60**, increase the cytotoxicity [64]. With the exception of **65**, each of the di-nuclear structures in **51**–**66** is disposed about a centre of inversion; in **51**, two independent molecules comprise the asymmetric unit, each being centrosymmetric. A representative molecule, with one of the more unusual dithiocarbamate di-anions covered in this survey, that is, of $(Me_2Sn)_2(L^{24})_2$ in (**54**), is shown in Figure 15a. Another unusual dithiocarbamate di-anion is present in $(Me_2Sn)_2(L^{26})_2$ (**56**), as shown in Figure 15b. The common feature of the tin-atom geometries of **54** and **56**, and indeed most of the structures conforming to the $(R_2Sn)_2(S_2CN\text{-spacer-}NCS_2)_2$ formula is the adoption of a skew-trapezoidal bipyramidal geometry. This arises as the co-planar dithiocarbamate residues coordinate in an asymmetric mode with the two longer Sn–S bonds lying to the same side of the skew-trapezoidal plane through the S_4 atoms. The tin-bound organo substituents lie over the weaker Sn–S bonds. There are three exceptions to this generalisation. In $(tBu)_2Sn(L^{18})_2$ in **63**, as shown in Figure 15c, one of the dithiocarbamate residues coordinates in a monodentate mode, so the coordination geometry is almost exactly intermediate between square-pyramidal and trigonal-bipyramidal. In each of $(Ph_2Sn)_2(L^{21})_2$ (**65**) and $(Ph_2Sn)_2(L^{32})_2$ in (**66**), as shown in Figure 15d, more symmetric modes of coordination of the dithiocarbamate residues are apparent, so the cis-C_2S_4 coordination geometries are distorted octahedral. Such perplexing coordination flexibility has been long recognised [91], especially as mono-nuclear diphenyltin bis(dithiocarbamate) molecules which are known to adopt both skew-trapezoidal bipyramidal and octahedral geometries in a ratio of 1:2, and therefore, the study of their structural characteristics continues to attract attention [92].

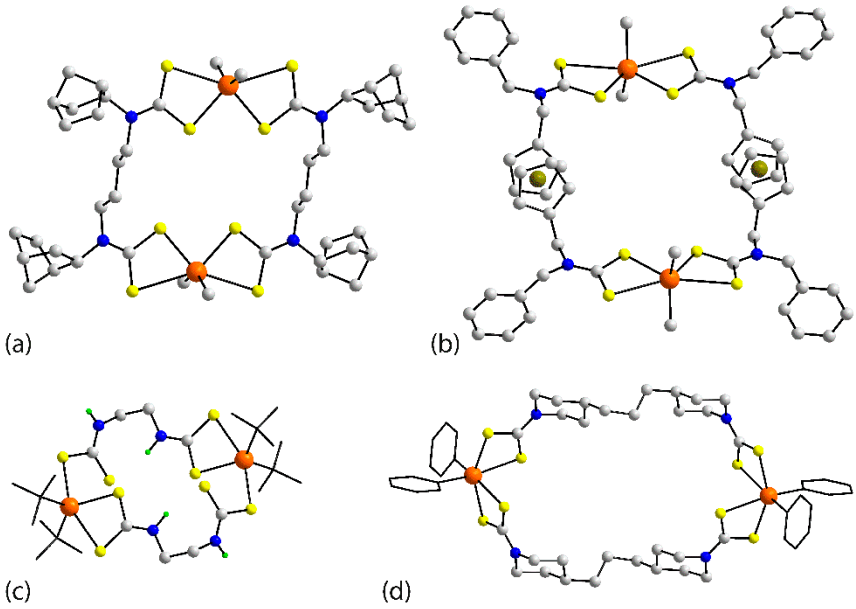

Figure 15. Molecular structures of (**a**) $(Me_2Sn)_2(L^{24})_2$ in the crystal of **54**, (**b**) $(Me_2Sn)_2(L^{26})_2$ in **56**, (**c**) $[(tBu)_2Sn]_2(L^{18})_2$ in **63**, and (**d**) $(Ph_2Sn)_2(L^{32})_2$ in **66**.

Despite having a different general formula to the preceding class of compounds, molecules of composition $(R_2SnX)_2(S_2CN\text{-spacer-}NCS_2)$ adopt very similar structural motifs in their crystals: $(Me_2SnCl)_2(L^1)$ in the crystal of **67** [68], $(Me_2SnCl)_2(L^{33})$ (**68**) [67], $(Me_2SnCl)_2(L^{34})$ (**69**) [69], $[(nBu)_2SnCl]_2(L^1)]$ (**70**) [68], $[(nBu)_2SnCl]_2(L^{32})$ (**71**) [70], $[(nBu)_2SnCl]_2(L^{34})$ (**72**) [69], $[(nBu)_2Sn]_2(L^{35})$ (**73**) [71], $(Ph_2SnCl)_2(L^2)$ (**74**) [72], $(Ph_2SnCl)_2(L^{32})$ (**75**) [70], $(Ph_2SnCl)_2(L^{36})$ (**76**) [73], and $[PhSn(X)CH_2Si(Me)_2C_6H_4C_6H_4Si(Me)_2CH_2Sn(Ph)X](L^2)$ for X = Cl (**77**) and X = I (**78**) [74]. However, by contrast to the $(R_2Sn)_2(S_2CN\text{-spacer-}NCS_2)_2$ molecules in crystals **51**-**66**, there is a significant diversity of symmetry in the 12 di-nuclear $(R_2SnX)_2(S_2CN\text{-spacer-}NCS_2)$ compounds: four have no crystallographically imposed symmetry, that is, **67**, Figure 16a, **71**, **74**, and **75**. Compounds **68**, as shown in Figure 16b, and **72** are generated by 2-fold symmetry, whereas compounds **69**, **70**, and **73**, as shown in Figure 16c, and **76** are disposed about a centre of inversion; molecules related to **73** attract interest as sensors for anions [71]. In each of **77**, as shown in Figure 16d, and **78**, where the tin-bound R groups are disparate and one pair of tin-bound R groups is connected, the molecules lack symmetry. The common features of the structures are an asymmetric mode of coordination of the dithiocarbamate residues and the presence of five-coordinate R_2S_2X-donor sets that are highly distorted from the ideal trigonal-bipyramidal and square-pyramidal extremes. However, owing to the presence of tin-bound electronegative X substituents in the molecular formula, $(R_2SnX)_2(S_2CN\text{-spacer-}NCS_2)$, the degree of asymmetry in the mode of coordination is somewhat reduced compared with that in the aforementioned $(R_2Sn)_2(S_2CN\text{-spacer-}NCS_2)_2$ molecules.

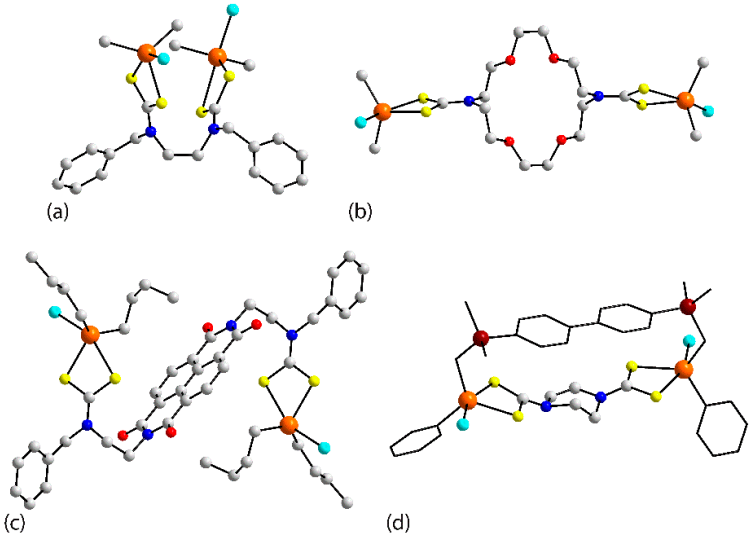

Figure 16. Molecular structures of (**a**) $(Me_2SnCl)_2(L^1)$ in the crystal of **67**, (**b**) $(Me_2SnCl)_2(L^{33})$ in **68**, (**c**) $[(nBu)_2Sn]_2(L^{35})$ in **73**, and (**d**) $[PhSn(Cl)CH_2Si(Me)_2C_6H_4C_6H_4Si(Me)_2CH_2Sn(Ph)Cl](L^2)$ in **77**.

The next category of molecular structures also resembles the preceding two classes and conforms to the general formula $(R_3Sn)_2(S_2C\text{-spacer-}CS_2)$. In all, there are 12 examples in this category: $(Cy_3Sn)_2(L^{37})$ in the crystal of **79** [75], $[(PhCH_2)_3Sn]_2(L^{32})$ (**80**) [70], $[(2\text{-}FC_6H_4CH_2)_3Sn]_2(L^2)$ (**81**) [76], $[(2\text{-}ClC_6H_4CH_2)_3Sn]_2(L^2)$ (**82**) [77], $[(Me_2(Ph)CCH_2)_3Sn]_2(L^2)$ (**83**) [78], $(Ph_3Sn)_2(L^2)$ (**84**) [79], $(Ph_3Sn]_2(L^2)$ (**85**) [80], $(Ph_3Sn)_2(L^2)$ (**86**) [81], $(Ph_3Sn)_2(L^{31})$ (**87**) [66], $(Ph_3Sn)_2(L^{32})$ (**88**) [70], $(Ph_3Sn)_2(L^{33})$ (**89**) [67], and $(Ph_3Sn)_2(L^{36})$ (**90**) [73]. The molecules are invariably di-nuclear with two representative examples being $(Ph_3Sn)_2(L^{31})$ in **87** and $(Ph_3Sn)_2(L^{36})$ in **90**, as illustrated in Figure 17. With the exception of **80**, **88**, and **90**, all of the aggregates are disposed about a centre of inversion; in **80**, two independent molecules comprise the asymmetric unit. The mode of coordination of the dithiocarbamate residues is to a first approximation considered monodentate, reflecting the reduced Lewis acidity of the tin atom centres in the triorganotin species compared with diorganotin species. The C_3S-donor sets are based on tetrahedra with distortions usually related to the close approach of the non-coordinating thione–sulphur atom. The molecule of **90** is of special interest as the presence of acidic hydroxyl–hydrogen atoms afford the opportunity of hydrogen-bond formation in the crystal. Indeed, each hydroxyl–hydrogen atom forms a hydrogen-bond to a thione–sulphur atom to form a linear, supramolecular tape.

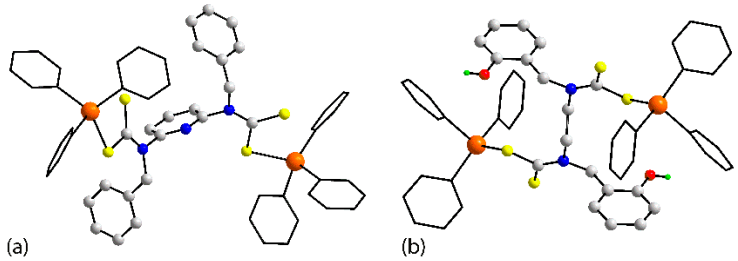

Figure 17. Molecular structures of (**a**) $(Ph_3Sn)_2(L^{31})$ in the crystal of **87** and (**b**) $(Ph_3Sn)_2(L^{36})$ in **90**.

In addition to cytotoxic **59** and **60**, [64], several organotin poly-dithiocarbamate compounds showed promising biological activities. Thus, **64** and **87** were tested, in vitro, for fungicidal activity and were found to display good anti-fungal activity towards *S. sclerotiorum* [66]. Furthermore, **71**, **75**, **80**, and **88** showed promising anti-leishmanial activities [70]. The cytotoxic activities of both **76** and **90** were assayed against two human tumour cell lines; that is, CoLo 205 (colon carcinoma cell) and Bcap37 (mammary tumour cell): the

diorganotin species **76** showed poor cytotoxic activity against the cell lines in comparison to the triorganotin derivative, **90** [73].

The six remaining organotin structures feature tri-functional dithiocarbamate ligands with four of these being $(Me_2SnCl)_3(L^{38})$ in the crystal of **91**, $(Me_2SnCl)_3(L^{39})$ (**92**), $[(tBu)_2SnCl]_2(L^{38})$ in (**93**) [68], and $(Ph_2SnCl)_2(L^{38})$ (**94**) [84]. Specific interest in these compounds, which were synthesised in situ, related to the development of metallo-supramolecular organotin assemblies. None of the tri-nuclear molecules have crystallographically imposed symmetry. As shown in Figure 18a, overall, the molecule in **91** has a bowl-shaped conformation, and this is also evident in each of **93** and **94**. By contrast, a somewhat flattened conformation is apparent for **92**, as shown in Figure 18b. The C_2ClS_2-donor sets define distorted geometries for the tin atoms as described above, that is, they are intermediate between square-pyramidal and trigonal-bipyramidal.

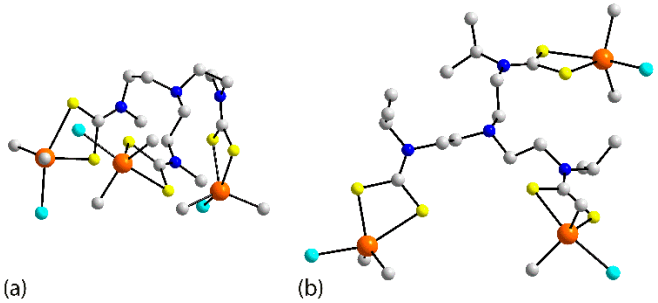

Figure 18. Molecular structures of (**a**) $(Me_2SnCl)_3(L^{38})$ in the crystal of **91** and (**b**) $(Me_2SnCl)_3(L^{39})$ in **92**.

The molecules of $(Ph_2Sn)_3(L^{39})_2$ in the crystal of **95** and $(Ph_2Sn)_3(L^{40})_2$ in **96** [82] are hexa-nuclear. Two views of **95** are given in Figure 19, one slightly off-set from the three-fold axis (the molecule is situated about a crystallographic site of symmetry 32 and the other, side-on). The overall molecule has the shape of a flattened capsule. A similar conformation is noted for $(Ph_2Sn)_3(L^{40})_2$ in **96**, which has crystallographic 3-fold symmetry. The coordination geometries are distorted octahedral, being based on cis-C_2S_4-donor sets.

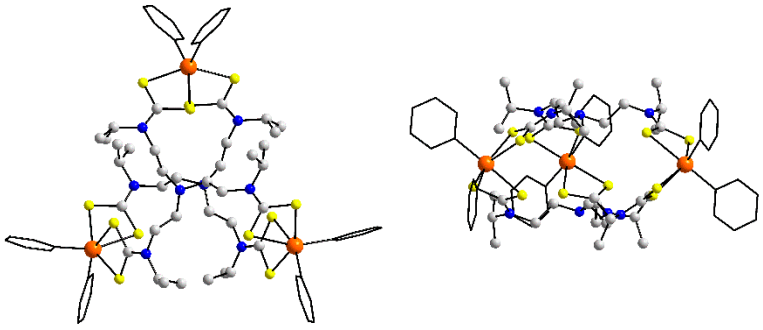

Figure 19. Two views of the molecular structure of $(Ph_2Sn)_3(L^{39})_2$ in the crystal of **95**.

In should be stressed here that comparisons of key geometric parameters formed by the poly-functional dithiocarbamate ligands with those formed by their mono-functional congeners indicate no definitive trends. This observation is entirely consistent with the results of density functional theory (DFT) calculations which indicate that little or no influence upon the electronic structure of the NCS_2^- chromophore is exerted by the nature of the N-bound alkyl substituents [93].

3.7. Coordination Chemistry of Lanthanide Poly-Dithiocarbamate Complexes

The motivation for studying lanthanide MOFs, LnMOFs, largely revolves around the luminescent properties of these materials [94] in recognition that such materials are

relatively unexplored. In this context, a series of tri-valent lanthanides were synthesised, each formulated as $\{(H_3O)[Ln(L^2)_2]\ 2.5(CH_3NO_2), 1.5(H_2O)\}_n$ for Ln = cerium (**97**), samarium (**98**), europium (**99**), gadolinium (**100**), terbium (**101**) [83], and neodymium (**102**) [84] with all six structures being isostructural; the compounds were synthesised from the reactions of $Ln(NO_3)_3.6H_2O$ (Ln = Ce, Sm, Eu, Gd, Tb and Nd) with an aqueous solution of $Na_2[L^2]$. Thus, it is the very last set of structures to be described in this overview that emphasises the potential of poly-functional dithiocarbamate ligands for the construction MOFs. As shown in Figure 20, the $\{[Nd(L^2)_2]^-\}_n$ anions in the crystal of **102** [84] assemble into a three-dimensional framework that defines square channels when viewed down the crystallographic *c*-axis; the framework is disordered by symmetry, and the channels are occupied by disordered cations and solvents. The L^2 di-anions are μ_2-bridging, chelating two neodymium(III) atoms, each of which is eight-coordinated within a distorted S_8-cube. In terms of photoluminescence properties, **98** exhibited well-resolved emission bands in the visible and near-infrared regions in comparison with the other materials [83].

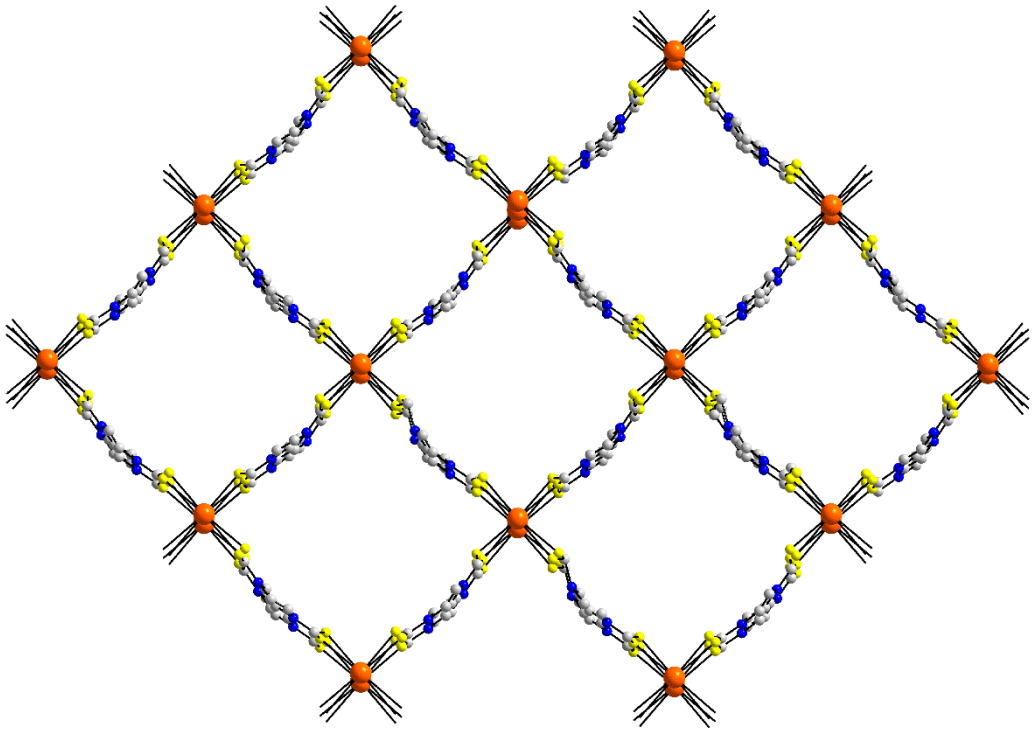

Figure 20. A view in projection down the *c*-axis of the three-dimensional framework defined by $\{[Nd(L^2)_2]^-\}_n$ anions in the crystal of **102**.

4. Conclusions

This survey of the crystallographic literature has revealed the utility of poly-functional dithiocarbamate ligands in forming multi-nuclear compounds of transition metals, main group elements, and lanthanides. The overwhelming majority of structures are zero-dimensional, ranging from a minimum of two atoms, as is commonly observed, to a maximum 36, the latter in a gold-rich cluster. Rare examples of one-, two-, and three-dimensional aggregation patterns are observed in the crystals. The diversity of poly-functional dithiocarbamate ligands is broad with 40 examples represented herein. All but three of these contain two $–CS_2^-$ residues with the exceptional examples having three $–CS_2^-$ residues. In all cases, all $–CS_2^-$ residues were engaged in coordination to a heavy element. The scope for increasing the range of poly-functional dithiocarbamate ligands with a variety of $–CS_2^-$ residues is limited only by the number of amine precursor molecules. The synthesis of the compounds is facile, usually relying on simple metathetical

reactions; often, the compounds may be prepared in situ without the need of isolating the poly-functional dithiocarbamate ligands themselves.

With the vast range of amine precursors available, the facile synthesis of the ligands and their heavy element compounds, opportunities in connecting lower dimensional aggregates into higher dimensional aggregation patterns via bridging pyridyl, and related molecules coupled with the potential applications, for example in the biomedical and materials fields, there is enormous scope for this branch chemistry, the exploration of which promises exciting discoveries.

Funding: Research in dithiocarbamate chemistry at Sunway University is funded by SUNWAY UNIVERSITY SDN BHD, grant number STR-RCTR-RCCM-001-2019. The APC was funded by Sunway University Sdn Bhd.

Institutional Review Board Statement: Not applicable.

Informed Consent Statement: Not applicable.

Data Availability Statement: Data sharing not applicable.

Conflicts of Interest: The authors declare no conflict of interest.

References

1. Hogarth, G. Transition metal dithiocarbamates: 1978–2003. In *Progress in Inorganic Chemistry*; Karlin, K.D., Ed.; John Wiley & Sons: Hoboken, NJ, USA, 2005; Volume 53, pp. 71–561. [CrossRef]
2. Debus, H. Ueber die Verbindungen der Sulfocarbaminsäure. *Justus Liebigs Ann. Chem.* **1850**, *73*, 26–34. [CrossRef]
3. Delépine, M. Metallic salts of dithiocarbamic acids; preparation of isothiocyanates in the aliphatic series. *Compt. Rend.* **1907**, *144*, 1125–1127.
4. Coucouvanis, D. The chemistry of the dithioacid and 1,1-dithiolate complexes. In *Progress in Inorganic Chemistry*; Lippard, S.J., Ed.; John Wiley & Sons: Hoboken, NJ, USA, 1970; Volume 11, pp. 234–371. [CrossRef]
5. Eisenberg, R. Structural systematics of 1,1- and 1,2-dithiolato chelates. In *Progress in Inorganic Chemistry*; Lippard, S.J., Ed.; John Wiley & Sons: Hoboken, NJ, USA, 1970; Volume 12, pp. 295–369. [CrossRef]
6. Coucouvanis, D. The chemistry of the dithioacid and 1,1-dithiolate complexes, 1968–1977. In *Progress in Inorganic Chemistry*; Lippard, S.J., Ed.; John Wiley & Sons: Hoboken, NJ, USA, 1979; Volume 26, pp. 301–469. [CrossRef]
7. Heard, P.J. Main group dithiocarbamate complexes. In *Progress in Inorganic Chemistry*; Karlin, K.D., Ed.; John Wiley & Sons: Hoboken, NJ, USA, 2005; Volume 53, pp. 1–69. [CrossRef]
8. Lee, S.M.; Heard, P.J.; Tiekink, E.R.T. Molecular and supramolecular chemistry of mono- and di-selenium analogues of metal dithiocarbamates. *Coord. Chem. Rev.* **2018**, *375*, 410–423. [CrossRef]
9. Cox, M.J.; Tiekink, E.R.T. The diverse coordination patterns in the structures of zinc, cadmium and mercury bis(1,1-dithiolates). *Rev. Inorg. Chem.* **1997**, *17*, 1–23. [CrossRef]
10. Tiekink, E.R.T. Molecular architecture and supramolecular association in the zinc-triad 1,1-dithiolates. Steric control as a design element in crystal engineering? *CrystEngComm* **2003**, *5*, 101–113. [CrossRef]
11. Tiekink, E.R.T. Aggregation patterns in the crystal structures of organometallic Group XV 1,1-dithiolates: The influence of the Lewis acidity of the central atom, metal- and ligand-bound steric bulk, and coordination potential of the 1,1-dithiolate ligands upon supramolecular architecture. *CrystEngComm* **2006**, *8*, 104–118. [CrossRef]
12. Tiekink, E.R.T.; Zukerman-Schpector, J. Stereochemical activity of lone pairs of electrons and supramolecular aggregation patterns based on secondary interactions involving tellurium in its 1,1-dithiolate structures. *Coord. Chem. Rev.* **2010**, *254*, 46–76. [CrossRef]
13. Tiekink, E.R.T. Exploring the topological landscape exhibited by binary zinc-triad 1,1-dithiolates. *Crystals* **2018**, *8*, 292. [CrossRef]
14. Tiekink, E.R.T. Perplexing coordination behaviour of potentially bridging bipyridyl-type ligands in the coordination chemistry of zinc and cadmium 1,1-dithiolate compounds. *Crystals* **2018**, *8*, 18. [CrossRef]
15. Ghasempour, H.; Wang, K.-Y.; Powell, J.A.; Karizi, F.Z.; Lv, X.-L.; Morsali, A.; Zhou, H.-C. Metal–organic frameworks based on multicarboxylate linkers. *Coord. Chem. Rev.* **2021**, *426*, 213542. [CrossRef]
16. Ko, M.; Mendecki, L.; Mirica, K.A. Conductive two-dimensional metal-organic frameworks as multifunctional materials. *Chem. Commun.* **2018**, *54*, 7873–7891. [CrossRef] [PubMed]
17. Cave, D.; Gascon, J.-M.; Bond, A.D.; Teat, S.J.; Wood, P.T. Layered metal organosulfides: Hydrothermal synthesis, structure and magnetic behaviour of the spin-canted magnet Co(1,2-(O_2C)(S)C_6H_4). *Chem. Commun.* **2002**, 1050–1051. [CrossRef] [PubMed]
18. Kusamoto, T.; Nishihara, H. Zero-, one- and two-dimensional bis(dithiolato) metal complexes with unique physical and chemical properties. *Coord. Chem. Rev.* **2019**, *380*, 419–439. [CrossRef]
19. Zeng, Q.; Wang, L.; Huang, Y.; Zheng, S.-L.; He, Y.; He, J.; Liao, W.-M.; Xu, G.; Zeller, M.; Xu, Z. An air-stable anionic two-dimensional semiconducting metal-thiolate network and its exfoliation into ultrathin few-layer nanosheets. *Chem. Commun.* **2020**, *56*, 3645–3648. [CrossRef]

20. Liebing, P.; Witzorke, J.; Oehler, F.; Schmeide, M. Dithiocarbamatocarboxylate (DTCC) ligands—Building blocks for hard/soft-heterobimetallic coordination polymers. *Inorg. Chem.* **2020**, *59*, 2825–2832. [CrossRef]
21. Gong, M.; Yang, J.; Li, Y.; Gu, J. Glutathione-responsive nanoscale MOFs for effective intracellular delivery of the anticancer drug 6-mercaptopurine. *Chem. Commun.* **2020**, *56*, 6448–6451. [CrossRef]
22. Xian, W.-R.; He, Y.; Diao, Y.; Wong, Y.-L.; Zhou, H.-Q.; Zheng, S.-L.; Liao, W.-M.; Xu, Z.; He, J. A bumper crop of boiling-water-stable metal–organic frameworks from controlled linker sulfuration. *Inorg. Chem.* **2020**, *59*, 7097–7102. [CrossRef]
23. Li, D.; Li, C.; Zhang, L.; Li, H.; Zhu, L.; Yang, D.; Fang, Q.; Qiu, S.; Yao, X. Metal-free thiophene-sulfur covalent organic frameworks: Precise and controllable synthesis of catalytic active sites for oxygen reduction. *J. Am. Chem. Soc.* **2020**, *142*, 8104–8108. [CrossRef]
24. Hsieh, J.; Chen, J.-Y.; Li, H.-Y.; Liu, H.-K.; Tu, H.-L.; Wang, C.-M. A thio-functionalized zinc phosphite with a large-channel framework and enhanced removal ability of mercury ion from aqueous solutions. *Dalton Trans.* **2020**, *49*, 11085–11089. [CrossRef]
25. Taylor, R.; Wood, P.A. A million crystal structures: The whole is greater than the sum of its parts. *Chem. Rev.* **2019**, *119*, 9427–9477. [CrossRef]
26. Bruno, I.J.; Cole, J.C.; Edgington, P.R.; Kessler, M.; Macrae, C.F.; McCabe, P.; Pearson, J.; Taylor, R. New software for searching the Cambridge Structural Database and visualizing crystal structures. *Acta Crystallogr. Sect. B Struct. Sci. Cryst. Eng. Mater.* **2002**, *58*, 389–397. [CrossRef] [PubMed]
27. Spek, A.L. checkCIF validation ALERTS: What they mean and how to respond. *Acta Crystallogr. Sect. E Crystallogr. Commun.* **2020**, *76*, 1–11. [CrossRef] [PubMed]
28. Brandenburg, K.; Berndt, M. *DIAMOND, Version 3.2k*; GbR: Bonn, Germany, 2006.
29. Unoura, K.; Abiko, Y.; Yamazaki, A.; Kato, Y.; Coomber, D.C.; Fallon, G.D.; Nakahara, K.; Bond, A.M. Synthesis, structure, and redox behaviour of a novel cis-dioxomolybdenum(VI) dinuclear complex with a quadradentate dithiocarbamate. *Inorg. Chim. Acta* **2002**, *333*, 41–50. [CrossRef]
30. Wilton-Ely, J.D.E.T.; Solanki, D.; Hogarth, G. Multifunctional dithiocarbamates as ligands towards the rational synthesis of polymetallic arrays: An example based on a piperizine-derived dithiocarbamate ligand. *Eur. J. Inorg. Chem.* **2005**, *20*, 4027–4030. [CrossRef]
31. Kovács, I.; Lebuis, A.-M.; Shaver, A. Ruthenium-assisted insertion of isothiocyanates into the silicon-sulfur bond: A comparative study on the reactivity of the S-Si and S-H Bonds in $CpRu(PPh_3)_2SX$ (X = H, Si^iPr_3) complexes. *Organometallics* **2001**, *20*, 35–41. [CrossRef]
32. Knight, E.R.; Cowley, A.R.; Hogarth, G.; Wilton-Ely, J.D.E.T. Bifunctional dithiocarbamates: A bridge between coordination chemistry and nanoscale materials. *Dalton Trans.* **2009**, 607–609. [CrossRef]
33. Knight, E.R.; Leung, N.H.; Lin, Y.H.; Cowley, A.R.; Watkin, D.J.; Thompson, A.L.; Hogarth, G.; Wilton-Ely, J.D.E.T. Multimetallic arrays: Symmetrical bi-, tri- and tetrametallic complexes based on the group 10 metals and the functionalisation of gold nanoparticles with nickel-phosphine surface units. *Dalton Trans.* **2009**, 3688–3697. [CrossRef]
34. Oliver, K.; White, A.J.P.; Hogarth, G.; Wilton-Ely, J.D.E.T. Multimetallic complexes of group 10 and 11 metals based on polydentate dithiocarbamate ligands. *Dalton Trans.* **2011**, *40*, 5852–5864. [CrossRef]
35. Beer, P.D.; Berry, N.G.; Cowley, A.R.; Hayes, E.J.; Oates, E.C.; Wong, W.W.H. Metal-directed self-assembly of bimetallic dithiocarbamate transition metal cryptands and their binding capabilities. *Chem. Commun.* **2003**, 2408–2409. [CrossRef]
36. Beer, P.D.; Cheetham, A.G.; Drew, M.G.B.; Fox, O.D.; Hayes, E.J.; Rolls, T.D. Pyrrole-based metallo-macrocycles and cryptands. *Dalton Trans.* **2003**, 603–611. [CrossRef]
37. Jantan, K.A.; Kwok, C.Y.; Chan, K.W.; Marchio, L.; White, A.J.P.; Deplano, P.; Serpe, A.; Wilton-Ely, J.D.E.T. From recovered metal waste to high-performance palladium catalysts. *Green Chem.* **2017**, *19*, 5846–5853. [CrossRef]
38. Torres-Huerta, A.; Höpfl, H.; Tlahuext, H.; Hernández-Ahuactzi, I.F.; Sánchez, M.; Reyes-Martínez, R.; Morales-Morales, D. Dinuclear macrocyclic palladium dithiocarbamates derived from the homologous series of aliphatic 1,x-diamines (x = 4–10). *Eur. J. Inorg. Chem.* **2013**, *2013*, 61–69. [CrossRef]
39. Webber, P.R.A.; Drew, M.G.B.; Hibbert, R.; Beer, P.D. Transition metal-directed self-assembly of calix[4]arene based dithiocarbamate ligands. *Dalton Trans.* **2004**, 1127–1135. [CrossRef] [PubMed]
40. Kumar, A.; Mayer-Figge, H.; Sheldrick, W.S.; Singh, N. Synthesis, structure, conductivity, and calculated nonlinear optical properties of two novel bis(triphenylphosphane)copper(I) dithiocarbamates. *Eur. J. Inorg. Chem.* **2009**, *2009*, 2720–2725. [CrossRef]
41. Huang, T.-H.; Yang, H.; Zhu, S.-L.; Zhao, B.; Yang, Y. Synthesis, structures and fluorescent properties of metal complexes based on polyphosphine ligands. *J. Mol. Struct.* **2017**, *1127*, 138–144. [CrossRef]
42. Beer, P.D.; Berry, N.; Drew, M.G.B.; Fox, O.D.; Padilla-Tosta, M.E.; Patell, S. Self-assembled dithiocarbamate-copper(II) macrocycles for electrochemical anion recognition. *Chem. Commun.* **2001**, 199–200. [CrossRef]
43. Cookson, J.; Evans, E.A.L.; Maher, J.P.; Serpell, C.J.; Paul, R.L.; Cowley, A.R.; Drew, M.G.B.; Beer, P.D. Metal-directed assembly of large dinuclear copper(II) dithiocarbamate macrocyclic complexes. *Inorg. Chim. Acta* **2010**, *363*, 1195–1203. [CrossRef]
44. Padilla-Tosta, M.E.; Fox, O.D.; Drew, M.G.B.; Beer, P.D. Self-assembly of a mixed-valence copper(II)/copper(III) dithiocarbamate catenane. *Angew. Chem., Int. Ed.* **2001**, *40*, 4235–4239. [CrossRef]
45. Fox, O.D.; Drew, M.G.B.; Beer, P.D. Resorcarene-based nanoarchitectures: Metal-directed assembly of a molecular loop and tetrahedron. *Angew. Chem. Int. Ed.* **2000**, *39*, 136–140. [CrossRef]

46. Guzei, I.A.; Spencer, L.C.; Lillywhite, S.; Darkwa, J. (μ-Piperazine-1,4-dicarbodithioato-$\kappa^4S^1,S^{1\prime}:S^4,S^{4\prime}$)bis[bis(triphenylphosphane-κP)gold(I)] chloroform disolvate. *Acta Crystallogr. Sect. E Crystallogr. Commun.* **2011**, *67*, m1629–m1630. [CrossRef]
47. Knight, E.R.; Leung, N.H.; Thompson, A.L.; Hogarth, G.; Wilton-Ely, J.D.E.T. Multimetallic arrays: Bi-, tri-, tetra-, and hexametallic complexes based on gold(I) and gold(III) and the surface functionalization of gold nanoparticles with transition metals. *Inorg. Chem.* **2009**, *48*, 3866–3874. [CrossRef] [PubMed]
48. Yu, S.-Y.; Sun, Q.-F.; Lee, T.K.-M.; Cheng, E.C.-C.; Li, Y.-Z.; Yam, V.W.-W. Au_{36} crown: A macrocyclization directed by metal-metal bonding interactions. *Angew. Chem., Int. Ed.* **2008**, *47*, 4551–4554. [CrossRef]
49. Jiang, X.-F.; Hau, F.K.-W.; Sun, Q.-F.; Yu, S.-Y.; Yam, V.W.-W. From $\{Au^I\cdots Au^I\}$-coupled cages to the cage-built 2-D $\{Au^I\cdots Au^I\}$ arrays: $Au^I\cdots Au^I$ bonding interaction driven self-assembly and their Ag^I sensing and photo-switchable behavior. *J. Am. Chem. Soc.* **2014**, *136*, 10921–10929. [CrossRef] [PubMed]
50. Sun, Q.-F.; Lee, T.K.-M.; Li, P.-Z.; Yao, L.-Y.; Huang, J.-J.; Huang, J.; Yu, S.-Y.; Li, Y.-Z.; Cheng, E.C.-C.; Yam, V.W.-W. Self-assembly of a neutral luminescent Au_{12} cluster with D_2 symmetry. *Chem. Commun.* **2008**, 5514–5516. [CrossRef] [PubMed]
51. Wang, Y.-Q.; Jiang, X.-F.; Li, H.; Yu, S.-Y. Self-assembly of a Au_{16} ring via metal–metal bonding interactions. *Chem. Asian J.* **2015**, *10*, 1146–1149. [CrossRef] [PubMed]
52. Yu, S.-Y.; Zhang, Z.-X.; Cheng, E.C.-C.; Li, Y.-Z.; Yam, V.W.-W.; Huang, H.-P.; Zhang, R. A Chiral luminescent Au_{16} ring self-assembled from achiral components. *J. Am. Chem. Soc.* **2005**, *127*, 17994–17995. [CrossRef] [PubMed]
53. Wong, W.W.H.; Curiel, D.; Lai, S.-W.; Drew, M.G.B.; Beer, P.D. Ditopic redox-active polyferrocenyl zinc(II) dithiocarbamate macrocyclic receptors: Synthesis, coordination and electrochemical recognition properties. *Dalton Trans.* **2005**, 774–781. [CrossRef] [PubMed]
54. Lai, S.-W.; Drew, M.G.B.; Beer, P.D. Metal-directed assembly of polyferrocenyl transition metal dithiocarbamate macrocyclic molecular boxes. *J. Organomet. Chem.* **2001**, *637–639*, 89–93. [CrossRef]
55. Wong, W.W.H.; Curiel, D.; Cowley, A.R.; Beer, P.D. Dinuclear zinc(II) dithiocarbamate macrocycles: Ditopic receptors for a variety of guest molecules. *Dalton Trans.* **2005**, 359–364. [CrossRef]
56. Fox, O.D.; Drew, M.G.B.; Wilkinson, E.J.S.; Beer, P.D. Cadmium- and zinc-directed assembly of nano-sized, resorcarene-based host architectures which strongly bind C_{60}. *Chem. Commun.* **2000**, 391–392. [CrossRef]
57. Lefton, J.B.; Kyle, B.; Pekar, K.B.; Runčevski, T. The crystal structure of Zineb, seventy-five years later. *Cryst. Growth Des.* **2020**, *20*, 851–857. [CrossRef]
58. Singh, N.; Kumar, A.; Prasad, R.; Molloy, K.C.; Mahon, M.F. Syntheses, crystal, photoluminescence and electrochemical investigation of some new phenylmercury(II) dithiocarbamate complexes involving ferrocene. *Dalton Trans.* **2010**, *39*, 2667–2675. [CrossRef] [PubMed]
59. Yadav, M.K.; Rajput, G.; Gupta, A.N.; Kumar, V.; Drew, M.G.B.; Singh, N. Exploring the coordinative behaviour and molecular architecture of new PhHg(II)/Hg(II) dithiocarbamate complexes. *Inorg. Chim. Acta* **2014**, *421*, 210–217. [CrossRef]
60. Guzmán-Percástegui, E.; Zakharov, L.N.; Alvarado-Rodríguez, J.G.; Carnes, M.E.; Johnson, D.W. Synthesis of a self-assembled Hg(II)-dithiocarbamate metallomacrocycle. *Cryst. Growth Des.* **2014**, *14*, 2087–2091. [CrossRef]
61. Santacruz-Juárez, E.; Cruz-Huerta, J.; Hernández-Ahuactzi, I.F.; Reyes-Martínez, R.; Tlahuext, H.; Morales-Rojas, H.; Höpfl, H. 24- and 26-membered macrocyclic diorganotin(IV) bis-dithiocarbamate complexes with N,N′-disubstituted 1,3- and 1,4-bis(aminomethyl)benzene and 1,1′-bis(aminomethyl)ferrocene as spacer groups. *Inorg. Chem.* **2008**, *47*, 9804–9812. [CrossRef]
62. Rojas-León, I.; Guerrero-Alvarez, J.A.; Hernández-Paredes, J.; Höpfl, H. Solvent-solvent and solvent-solute interactions in a 3D chloroform clathrate with diorganotin macrocycles in the nano-sized pores. *Chem. Commun.* **2012**, *48*, 401–403. [CrossRef] [PubMed]
63. Reyes-Martínez, R.; Mejia-Huicochea, R.; Guerrero-Alvarez, J.A.; Höpfl, H.; Tlahuext, H. Synthesis, heteronuclear NMR and X-ray crystallographic studies of two dinuclear diorganotin(IV) dithiocarbamate macrocycles. *ARKIVOC* **2008**, 19–30. [CrossRef]
64. Selvaganapathi, P.; Thirumaran, S.; Ciattini, S. Synthesis, spectra, crystal structures and anticancer studies of 26-membered macrocyclic dibutyltin(IV) dithiocarbamate complexes: Single-source precursors for tin sulfide nanoparticles. *Appl. Organomet. Chem.* **2019**, *33*, e5089. [CrossRef]
65. Jung, O.S.; Sohn, Y.S.; Ibers, J.A. Synthesis and properties of some ethylenebis(dithiocarbamate) diorganotin(IV) complexes. The structure of $[(tert\text{-}Bu)_2Sn(ebdtc)]_2$.4THF [tetra-tert-butylbis(ethylenebis(dithiocarbamato)ditin.tetrakis(tetrahydrofuran)]. *Inorg. Chem.* **1986**, *25*, 2273–2275. [CrossRef]
66. Yu, Y.; Yang, H.; Wei, Z.-W.; Tang, L.-F. Synthesis, structure, and fungicidal activity of organotin dithiocarbamates derived from pyridinamines and aryl diamines. *Heteroat. Chem.* **2014**, *25*, 274–281. [CrossRef]
67. Celis, N.A.; Villamil-Ramos, R.; Höpfl, H.; Hernández-Ahuactzi, I.F.; Sánchez, M.; Zamudio-Rivera, L.S.; Barba, V. Dinuclear monomeric and macrocyclic organotin dithiocarbamates derived from 1,10-diaza-18-crown-6 and 4,4′-trimethylenedipiperidine. *Eur. J. Inorg. Chem.* **2013**, *2013*, 2912–2922. [CrossRef]
68. Tlahuext, H.; Reyes-Martínez, R.; Vargas-Pineda, G.; López-Cardoso, M.; Höpfl, H. Molecular structures and supramolecular association of chlorodiorganotin(IV) complexes with bis- and tris-dithiocarbamate ligand. *J. Organomet. Chem.* **2011**, *696*, 693–701. [CrossRef]
69. Santacruz-Juárez, E.; Cruz-Huerta, J.; Torres-Huerta, A.; Hernández-Cruz, M.G.; Barba, V.; Tlahuext, H.; Höpfl, H. Stabilization of $[(n Bu_2SnCl)(\mu\text{-}Cl)_2(ClSn n Bu_2)]$ within the solid-state structure of a chlorodi-*n*-butyltin(IV) dithiocarbamate. *J. Organomet. Chem.* **2014**, *770*, 121–129. [CrossRef]

70. Ali, S.; Zia-ur-Rehman; Muneeb-ur-Rehman; Khan, I.; Shah, S.N.A.; Ali, R.F.; Shah, A.; Badshah, A.; Akbar, K.; Bélanger-Gariepy, F. New homobimetallic organotin(IV) dithiocarbamates as potent antileishmanial agents. *J. Coord. Chem.* **2014**, *67*, 3414–3430. [CrossRef]
71. Rodríguez-Uribe, N.A.; Claudio-Catalán, M.Á.; Medrano, F.; Pina Luis, G.; Tlahuext, H.; Godoy-Alcántar, C. Anion interaction with homoditopic chlorodiorganotin(IV) dithiocarbamate complexes derived from a naphthalene diimide. A pathway to obtain metallamacrocycles. *Polyhedron* **2020**, *186*, 114615. [CrossRef]
72. Fuentes-Martínez, J.P.; Toledo-Martínez, I.; Román-Bravo, P.; García y García, P.; Godoy-Alcántar, C.; López-Cardoso, M.; Morales-Rojas, H. Diorganotin(IV) dithiocarbamate complexes as chromogenic sensors of anion binding. *Polyhedron* **2009**, *28*, 3953–3966. [CrossRef]
73. Tian, L.; Zheng, X.; Zheng, X.; Sun, Y.; Yan, D.; Tu, L. Synthesis, structure and cytotoxic activity of binuclear phenyltin(IV) complexes with *N*,*N*′-bis(2-hydroxybenzyl)-1,2-ethanebis(dithiocarbamate) ligand. *Appl. Organomet. Chem.* **2011**, *25*, 785–790. [CrossRef]
74. Rojas-León, I.; Alnasr, H.; Jurkschat, K.; Vasquez-Ríos, M.G.; Gómez-Jaimes, G.; Höpfl, H.; Hernández-Ahuactzí, I.F.; Santillan, R. Formation of metal-based 21- and 22-membered macrocycles from dinuclear organotin tectons and ditopic organic ligands carrying carboxylate or dithiocarbamate groups. *Organometallics* **2019**, *38*, 2443–2460. [CrossRef]
75. Cotero-Villegas, A.M.; Pérez-Redondo, M.d.C.; López-Cardoso, M.; Toscano, A.; Cea-Olivares, R. Organotin(IV) azepane dithiocarbamates: Synthesis and characterization of the first organotin(IV) complexes with seven-membered cyclic dithiocarbamates. *Phosphorus, Sulfur, Silicon Relat. Elem.* **2020**, *195*, 498–506. [CrossRef]
76. Yin, H.-D.; Wang, C.-H.; Xing, Q.-J. Synthesis and molecular structure of binuclear organotin complex bridged by piperazinyl-bidithiocarbamate anion. *Jiegou Huaxue* **2004**, *23*, 490–493.
77. Yin, H.; Wang, C. Bis[tri(o-chlorobenzyl)tin(IV)] piperazinylbisdithiocarbamate. *Appl. Organomet. Chem.* **2004**, *18*, 145–146. [CrossRef]
78. Tian, L.; Shang, Z.; Yu, Q.; Li, D.; Yang, G. Bis[tris(2-methyl-2-phenylpropyl)tin]-piperazinyldithiocarbamate. *Appl. Organomet. Chem.* **2004**, *18*, 253–254. [CrossRef]
79. Poplaukhin, P.; Tiekink, E.R.T. (μ-Piperazine-1,4-dicarbodithioato-$\kappa^4S,S':S'',S'''$)bis[triphenyltin(IV)] dichloromethane solvate. *Acta Crystallogr. Sect. E Crystallogr. Commun.* **2008**, *64*, m1177. [CrossRef] [PubMed]
80. Yin, H.-D.; Ma, C.-L.; Wang, Y.; Fang, H.-X.; Shao, J.-X. Synthesis and crystal structure of binuclear organotin(IV) complexes $[Ph_3Sn(CH_3OH)O_2CC_6H4CO_2(CH_3OH)SnPh_3]\cdot 2CH_3OH$ and $[Ph_3SnS_2CN(CH_2CH_2)_2NCS_2SnPh_3]\cdot 2CH_3OH$. *Huaxue Xuebao* **2002**, *60*, 897–903.
81. Yin, H.; Deng, B.; Ma, C. Spectroscopic properties and crystal structure of bis[triphenyltin(IV)] piperazine bis(dithiocarbamate). *Fenxi Ceshi Xuebao* **2004**, *23*, 23–26.
82. Reyes-Martínez, R.; García y García, P.; López-Cardoso, M.; Höpfl, H.; Tlahuext, H. Self-assembly of diphenyltin(IV) and tris-dithiocarbamate ligands to racemic trinuclear cavitands and capsules. *Dalton Trans.* **2008**, 6624–6627. [CrossRef]
83. Wang, S.; Xu, J.; Wang, J.; Wang, K.-Y.; Dang, S.; Song, S.; Liu, D.; Wang, C. Luminescence of samarium(III) bis-dithiocarbamate frameworks: Codoped lanthanide emitters that cover visible and near-infrared domains. *J. Mater. Chem. C* **2017**, *5*, 6620–6628. [CrossRef]
84. Xu, J.; Liu, T.; Han, X.; Wang, S.; Liu, D.; Wang, C. Construction of a porous three dimensional rare earth metal–sulfur-ligand open framework. *Chem. Commun.* **2015**, *51*, 15819–15822. [CrossRef]
85. Schmidbaur, H. Supramolecular chemistry. Going for gold. *Nature* **2001**, *413*, 31–33. [CrossRef]
86. Schmidbaur, H.; Schier, A. A briefing on aurophilicity. *Chem. Soc. Rev.* **2008**, *37*, 1931–1951. [CrossRef]
87. Tiekink, E.R.T. Supramolecular assembly of molecular gold(I) compounds: An evaluation of the competition and complementarity between aurophilic (Au· · ·Au) and conventional hydrogen bonding interactions. *Coord. Chem. Rev.* **2014**, *275*, 130–153. [CrossRef]
88. Cox, M.J.; Tiekink, E.R.T. Structural features of zinc(II) bis(*O*-alkyldithiocarbonate) and zinc(II) bis(*N*,*N*-dialkyldithiocarbamate) compounds. *Z. Kristallogr.* **1999**, *214*, 184–190. [CrossRef]
89. Guardiola, F.A.; Cuesta, A.; Meseguer, J.; Esteban, M.A. Risks of using antifouling biocides in aquaculture. *Int. J. Mol. Sci.* **2012**, *13*, 1541–1560. [CrossRef] [PubMed]
90. Jotani, M.M.; Tan, Y.S.; Tiekink, E.R.T. Bis[bis(*N*-2-hydroxyethyl,*N*-isopropyldithiocarbamato)mercury(II)]$_2$: Crystal structure and Hirshfeld surface analysis. *Z. Kristallogr. Cryst. Mater.* **2016**, *231*, 403–413. [CrossRef]
91. Tiekink, E.R.T. Tin dithiocarbamates: Applications and structures. *Appl. Organomet. Chem.* **2008**, *22*, 533–550. [CrossRef]
92. Haezam, F.N.; Awang, N.; Kamaludin, N.F.; Jotani, M.M.; Tiekink, E.R.T. (*N*,*N*-Diallyldithiocarbamato-κ^2S,S')triphenyltin(IV) and bis(*N*,*N*-diallyldithiocarbamato-κ^2S,S')diphenyltin(IV): Crystal structure, Hirshfeld surface analysis and computational study. *Acta Crystallogr., Sect. E: Crystallogr. Commun.* **2020**, *76*, 167–176. [CrossRef]
93. Tiekink, E.R.T.; Hall, V.J.; Buntine, M.A. An examination of the influence of crystal structure on molecular structure. The crystal and molecular structures of some diorganotinchloro-(*N*,*N*-dialkyl-dithiocarbamate)s, R2Sn(S2CNR′2)Cl, R = Me, *t*Bu, Ph, Cy; R′2 = (Et)2, (Et, Cy) and (Cy)2: A comparison between solid state and theoretical structures. *Z. Kristallogr.* **1999**, *214*, 124–134. [CrossRef]
94. Cui, Y.; Chen, B.; Qian, G. Lanthanide metal-organic frameworks for luminescent sensing and light-emitting applications. *Coord. Chem. Rev.* **2014**, *273–274*, 76–86. [CrossRef]